Friction https://mc03.manuscriptcentral.com/friction
https://doi.org/10.26599/FRICT.2026.9441220

Review

Lubrication theory, tribological characteristics, and performance enhancement strategies of hydrodynamic thrust bearings: comprehensive review

Tao Zhao[1], Bo Xu[2, 3], Bing Xue[2, 3], Tao Wang[2, 3], Yongbo Li[2, 3], Zhi Zhang[2, 3], Youqiang Wang[1, 4]✉

[1] School of Mechanical and Automotive Engineering, Qingdao University of Technology, Qingdao 266520, China

[2] China Yangtze Power Co., Ltd, Yichang 443000, China.

[3] Hubei Technology Innovation Center for Smart Hydropower, Wuhan 430010, China

[4] Key Lab of Industrial Fluid Energy Conservation and Pollution Control, Ministry of Education Qingdao 266520, China

✉ Corresponding author. E-mail: wyq1970301@126.com

Received: September 25, 2025; Revised: December 25, 2025; Accepted: January 26, 2026

Research Funding: China Yangtze Power Co., Ltd. (Contract No. Z152402042)

Abstract: As key supporting components in large-scale equipment, the lubrication performance of hydrodynamic thrust bearings directly determines the operational efficiency, stability and service life of the entire mechanical system. With the rapid development of modern industry, the demand for complex working conditions poses severe challenges to the lubrication systems of hydrodynamic thrust bearings, making the accurate evaluation and prediction of their friction and lubrication behaviors a critical technical issue in the field of mechanical engineering. This paper systematically summarizes the research progress of lubrication theories for hydrodynamic thrust bearings, covering the evolutionary process from early hydrodynamic (HD) lubrication theory to thermoelastic hydrodynamic (TEHD) lubrication theory that integrates thermal and elastic effects, and highlights the breakthroughs of computational fluid dynamics (CFD) technology in simulating complex flow fields. Concurrently, recent advances in thrust bearing performance testing technologies are summarized, which include fundamental tribological tests and bearing model test rigs, with detailed discussion on the progress in monitoring key parameters such as oil film pressure, thickness, and temperature. Performance enhancement strategies are systematically elaborated from two primary perspectives: the improvement of thrust bearing liner materials and the optimization of surface textures. Finally, by comprehensively analyzing existing research, future research directions are outlined, emphasizing the development of high-fidelity multi-physics coupling models, the integration of multi-sensor-integrated distributed dynamic measurement with algorithmic innovation, and the synergistic design and optimization of materials and surface textures. This paper aims to provide a systematic reference for the design, performance improvement, and cutting-edge research of hydrodynamic thrust bearings under complex working conditions.

Keywords: hydrodynamic thrust bearings; lubrication theory; test technologies; liner materials; surface texture; friction and wear

1 Introduction

Hydrodynamic thrust bearings, as core components for force and motion transmission in high-end equipment, are widely applied in key fields such as aerospace, hydropower energy, marine propulsion, and nuclear power. Their lubrication performance directly determines the operational efficiency, stability, and service life of mechanical systems [1]. With the rapid development of modern industry, driven by technical demands for high speed, heavy load, and complex working conditions, bearing lubrication systems need to balance multi-dimensional performance indicators including oil film load-carrying capacity, temperature control, and friction loss. Relevant studies not only need to reveal the mechanisms of oil film formation and evolution but also address key issues such as multi-physical field coupling and accurate performance prediction under complex working conditions [2-4]. Therefore, hydrodynamic thrust bearings have attracted extensive attention in both academic and engineering fields. Accurately evaluating and predicting their lubrication behavior and service performance under actual working conditions has become a critical technical challenge urgently needing breakthrough in the current field of mechanical engineering.

Nomenclature

CHTC	Convective heat transfer coefficient	Φ	Diameter
H	The CHTC of the bearing pad main surface	D	Depth
H_c	The CHTC at the outer angle of the trailing edge	S	Spacing
h_c const	Uniform CHTC	Q	Quantity
h_c var	Non-uniform CHTC	W	Width
F	Average CHTC	L	Length
U	Local sliding speed	λ	The groove depth ratio
η_{ch}	Bulk viscosity of the lubricant	NSGA-II-RSM	NSGA-II multi-objective optimization method based on the response surface methodology
B	Arc length of pad at mean radius	SAA	Simulated annealing algorithm
ω	Angular velocity	BP-IMOALA	BP neural network-based improved multi-objective ant lion algorithm
β	Turbulent transition factor	BP-IMODA	BP neural network-based improved multi-objective dragonfly algorithm
P_r	Prandtl number	BP-IMOSSA	BP neural network-based improved multi-objective salp swarm algorithm
ε_m	Eddy diffusivity	PSO	Particle swarm optimization
GA-SQP	GA-sequential quadratic programming	NSGA-II	Non-dominated sorting genetic algorithm II
FSI	Fluid-structure interaction	MO-ASMO	Multi-objective adaptive surrogate model optimization
FEM	Finite element method	FDM	Finite difference method

Hydrodynamic thrust bearings operate on the principle of forming a wedge-shaped gap between the thrust collar and pads, which generates a hydrodynamic oil film to support the axial load. In actual operation, hydrodynamic thrust bearings face multiple challenges and failure risks under complex operating conditions. At high speeds, heat generation due to viscous shear within the oil film can lead to excessive local temperature rises, which reduces lubricant viscosity, destabilizes the oil film thickness, and ultimately accelerates friction and wear between the bearing pads and the collar [5, 6]. Under heavy loads, mechanical and thermal deformations of the pads and thrust collar can alter the oil film distribution, resulting in uneven load sharing and potentially catastrophic failures such as pad burnout [7]. These issues have driven the evolution of lubrication theory from early simplified models to TEHD models that integrate thermal effects and elastic deformation. In recent years, lubrication modeling methods based on multi-physical field coupling have gradually become a research hotspot. These models have incorporated various key factors such as shaft misalignment, turbulent effects, cavitation phenomena, surface roughness, and thermoelastic deformation [8-10]. Furthermore, CFD technology has been employed to achieve accurate simulation of complex flow fields [11, 12], which not only reflects complex lubrication behaviors more realistically but also significantly expands the applicable boundaries of traditional theories. These models have systematically revealed the mechanisms of lubricating film formation, pressure distribution laws, temperature field evolution, and their influence mechanisms on bearing lubrication performance, providing a solid theoretical basis for the design calculation and structural optimization of sliding bearings.

Experimental research serves as a critical bridge between theory and engineering practice, establishing a comprehensive verification system from microscopic mechanisms to macroscopic performance. Fundamental tribological experiments focus on microscopic frictional behavior of material surfaces, investigating intrinsic characteristics such as wear mechanisms of different structures and materials, and the principles of lubricating film formation [13, 14]. Bearing model tests, by simulating conditions such as rotational speed and load under actual working conditions, systematically evaluate the operational performance of bearings [15, 16]. These experiments not only provide essential data for calibrating and verifying theoretical models but also drive theoretical advances through the analysis of complex experimental phenomena, laying an experimental foundation for the performance optimization and engineering application of thrust bearings.

Reasonable selection of materials and structural optimization are instrumental in enhancing the performance of thrust bearings. Thrust bearing failure usually starts with material damage and the consequent damage to related components, thus imposing high requirements on bearing pad materials. For large thrust bearings operating under heavy loads, babbitt metals and polymers are the primary materials used for bearing pads [17, 18]. Driven by industrial demands for higher performance and efficiency, polymer materials have increasingly supplanted babbitt metals and have become a major focus of research. Surface texturing is an effective technology for enhancing the performance of thrust bearings. It can significantly improve their tribological properties (reducing friction and wear), while also increasing load-carrying capacity and lubrication state [19-21]. Current research mainly investigates textured thrust bearings from aspects such as operating parameters, texture shape, texture layout position, and texture parameters.

Based on the above analysis, this paper systematically summarizes the development process of lubrication theory for thrust bearings, and discusses the application breakthroughs of CFD technology in simulating complex flow fields. Clarifies the technical progress of fundamental tribological experiments and bearing model tests. Explores in depth the performance differences of bearing pad lining materials and the influence of surface texture on lubrication characteristics, and summarizes the application of numerical optimization algorithms in texture design. This paper aims to summarize the current progress and existing challenges in aspects such as adaptability to complex working conditions, model prediction accuracy, and experimental verification systems, so as to provide a reference for promoting the performance improvement and engineering application of thrust bearings under different working conditions. The framework of this article is shown in **Fig. 1**.

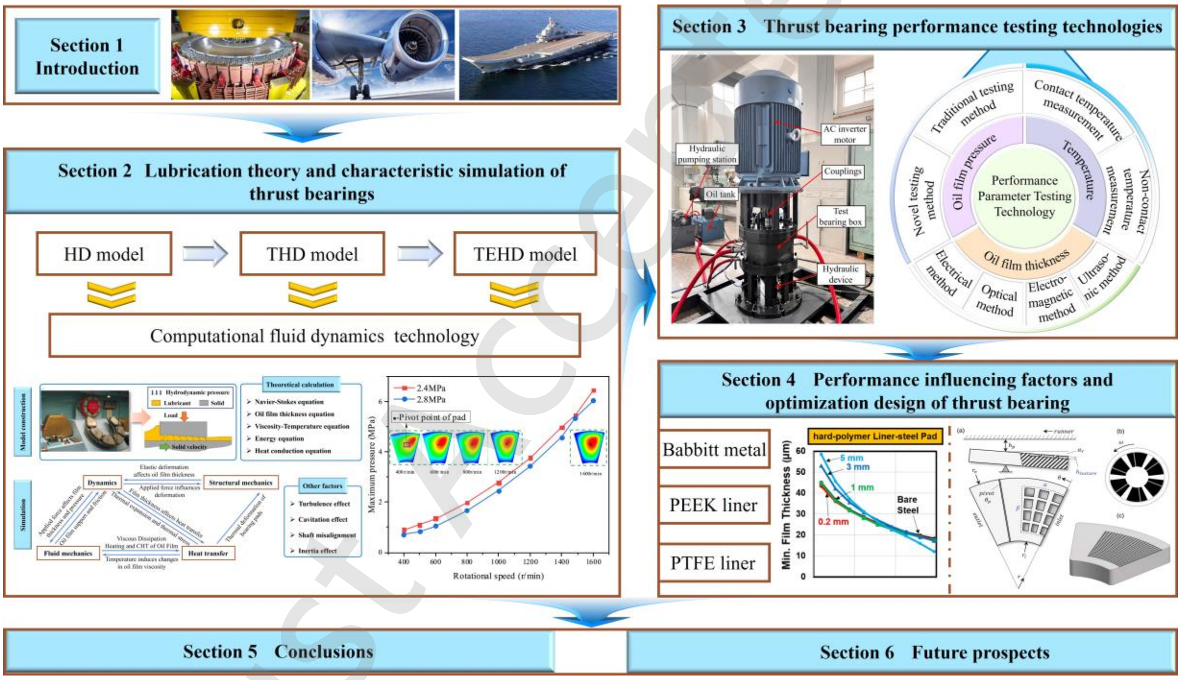

Fig. 1 The framework of this paper

2 Lubrication theory and characteristic simulation of thrust bearings

The development of lubrication theory for thrust bearings traces back to Newton's definition of fluid viscosity in the 17th century, which laid the foundation for subsequent research on fluid lubrication. However, systematic studies on lubrication theory did not emerge until the late 19th century. Between 1883 and 1885, B. Tower [22] conducted experiments on railway axle sliding bearings and became the first to observe hydrodynamic pressure in the bearing oil film, proposing the hydrodynamic oil film theory. In 1886, Reynolds [23] simplified the Navier-Stokes equations (N-S equations) based on hydrodynamic principles and derived the Reynolds equation to describe the pressure distribution within the oil film. Under the assumptions of laminar flow, incompressible fluids, small inertial forces, smooth surfaces, and isothermal flow, this equation established the fundamental framework of modern fluid lubrication theory. In the 1940s, Christopherson et al. [24] proposed a HD analysis model, which calculates oil film flow characteristics under isothermal assumptions. Although this model is limited by significant deviations from experimental measurements, it provided a new approach for analyzing the performance of hydrodynamic thrust bearings.

The limitation of classical lubrication theory lies in the disconnection between idealized assumptions and actual working conditions, manifested in neglecting non-isothermal effects and thermorheological properties, failing to consider the influence of surface roughness and turbulent flow, and lacking descriptions of multi-physical field coupling. Subsequent research has progressively overcome these constraints by introducing TEHD lubrication theory, incorporating temperature-dependent rheological parameters, developing numerical simulation methods such as the FEM, and establishing multiscale coupling models. These advances have promoted the evolution of lubrication theory toward accurate prediction under unsteady, non-isothermal, and complex operating conditions. The historical development of hydrodynamic lubrication theory for thrust bearings is illustrated in **Fig. 2**.

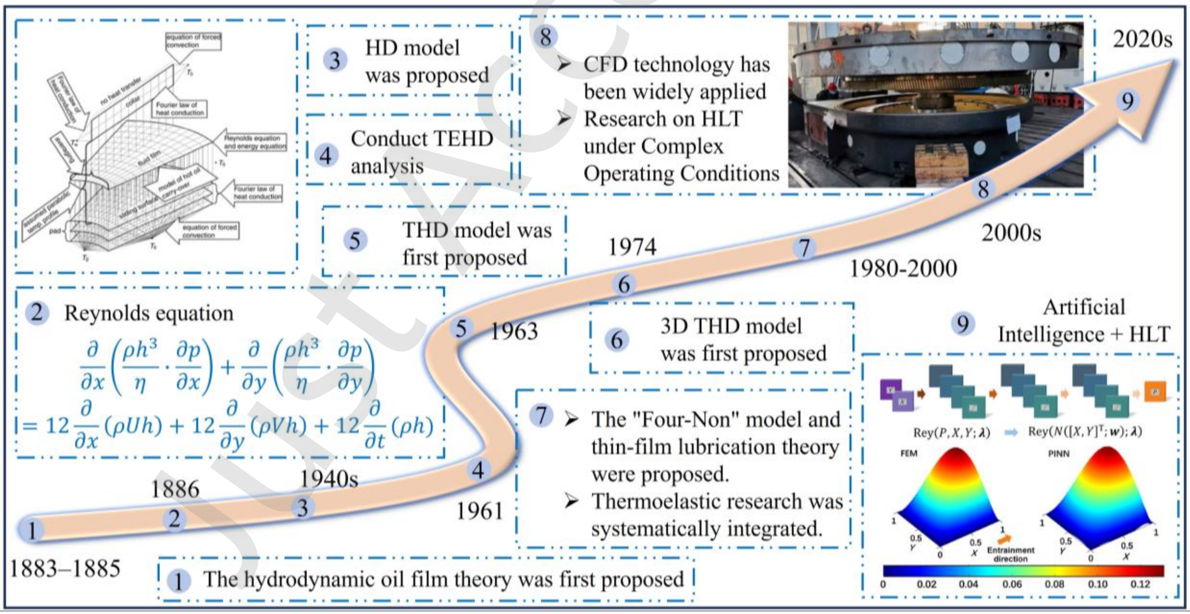

Fig. 2 The evolutionary history of hydrodynamic lubrication theory for thrust bearings

2.1 Thermohydrodynamic (THD) lubrication analysis based on the Reynolds equation

THD builds on HD by considering the influence of temperature on viscosity and thermal effects such as viscous shear heat and heat conduction. The development of THD stems from the limitations of HD in explaining engineering issues like overheating failure of high-speed bearings. In the mid-20th century, as the demand for lubrication performance in equipment such as aero-engines increased, the "isothermal assumption" of HD could no longer meet practical needs, prompting scholars to conduct research on thermal effects inside bearings [25, 26]. In 1963, Dowson et al. [27, 28] proposed the " THD model" and solved the Reynolds equation, energy equation, and viscosity-temperature equation within the oil film simultaneously. It was concluded that the heat generated by viscous shear stress in the oil film reduces the viscosity and density of the lubricating oil, thereby decreasing the oil film thickness. Research on THD evolved from 1D and 2D thermal correction models to the 3D THD model proposed by Huebnler [29] in 1974, which achieved full coupling analysis of the circumferential, radial, and axial temperature fields of the oil film as well as solid heat conduction. Theoretical analysis indicates that the 3D THD model established based on adiabatic theory is closer to the actual working state of thrust bearings than the 2D THD model [30].

Depending on whether the structural field is considered, THD models can be categorized into the following two types: The first type involves only the oil film domain, where the interface between the oil film and structural components is set as an adiabatic boundary. The second type establishes both the oil film domain and the solid domain, solving the Reynolds equation and energy equation for the oil film as well as the heat conduction equation for the solid domain, with heat conservation maintained at the interface between the two domains. Liu [31] conducted a 2D THD analysis on thrust bearings of hydro-turbine units, discussing the relationship between thrust load and minimum oil film thickness. However, heat conduction was not considered in his research, resulting in a higher calculated oil film temperature than the actual one. Wang et al. [32] established a 2D adiabatic THD model incorporating vibration frequency, solved the axial oil film stiffness and damping via the perturbation method and FDM. The study revealed that under the 30,000 N operating condition, the discrepancy between the theoretical and experimental results of axial oil film stiffness was no more than 7%, exhibiting good accuracy. However, as the load increased to the heavy-load condition of 44,000 N, this discrepancy rises significantly to the range of 30%–83%. In addition, the theoretical estimation of axial oil film damping also exhibited considerable discrepancies with the experimental results. The 3D THD model constructed by Almqvist et al. [33] considered the 3D temperature field distribution of the oil film and bearing pads as well as the 2D temperature gradient of the rotor, set viscosity and density as functions of temperature and pressure, calibrated boundary parameters such as hot oil carry-over layer thickness and heat transfer coefficient through experiments, and confirmed that, for general cases, this model can accurately analyze the lubrication performance of thrust bearings under laminar flow conditions, as shown in **Fig. 3**. Wasilczuk [34] established a 3D THD model of thrust bearings considering cavitation effect and heat transfer between the oil film and solid domain, set the minimum film thickness and maximum temperature as optimization constraints, constructed an objective function incorporating safe operation indicators for oil film profile optimization. Jiang [35] achieved heat transfer between the fluid domain and solid domain by coupling the energy equation with the solid heat conduction equation and combining boundary conditions of continuous interfacial heat flux and equal temperature, then explored the effects of load, rotational speed, oil type, and bearing pad material on bearing lubrication performance through THD analysis.

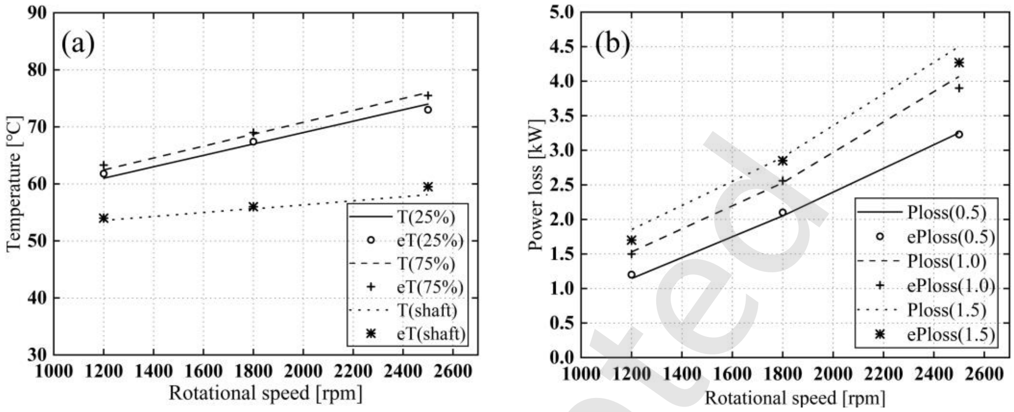

Fig. 3 Comparison between theory and experiment[33]. (a) Under 1.0 MPa load, temperatures at shaft center and runner (at 25% and 75% of pad width) versus rotational speed. (b) Bearing power loss versus rotational speed at the loads 0.5, 1.0, and 1.5 MPa, respectively.

2.2 TEHD analysis based on the Reynolds equation

With the trend towards high-speed and heavily loaded thrust bearings, the THD model has become inadequate for engineering requirements due to its neglect of solid component deformation. This has driven the development and application of TEHD theory [36] Theoretical and experimental comparisons indicate that the TEHD model more accurately reflects the actual operational state of the bearing. Under identical operating conditions, the maximum pad temperature predicted by the THD model is approximately 3-4℃ higher than that predicted by the TEHD model, while its predicted maximum oil film thickness (19.64 μm) is also significantly lower than the TEHD result (42.83 μm). This underestimation of film thickness causes the THD model to overestimate the axial stiffness and damping coefficients by approximately 38% and 61%, respectively [37].

The TEHD model account for elastic deformation induced by oil film pressure and thermal deformation resulting from viscous shear heating. These two deformation mechanisms modify the oil film thickness distribution, thereby affecting the lubrication performance of the bearing [38, 39]. Analysis indicates that considering only elastic deformation leads to an underestimation of the oil film pressure peak, while considering only thermal deformation results in an overestimation. However, TEHD models considering either deformation mechanism alone demonstrate higher prediction accuracy for key lubrication parameters than the THD model [40]. More importantly, the deformation effect exhibits significant nonlinear characteristics under heavy load conditions. Once the load exceeds a certain threshold, drastic changes in bearing performance parameters may occur with only a slight increase in load. This behavior represents a critical potential risk factor for pad overheating and even failure [41]. In summary, the lubrication of thrust bearings is inherently a complex issue involving fluid-solid-thermal multi-field coupling. By systematically coupling the flow field, solid deformation, and heat transfer processes, the TEHD model provides a more reliable theoretical foundation for thrust bearing performance analysis. A summary of TEHD analysis for thrust bearings is presented in Table 1.

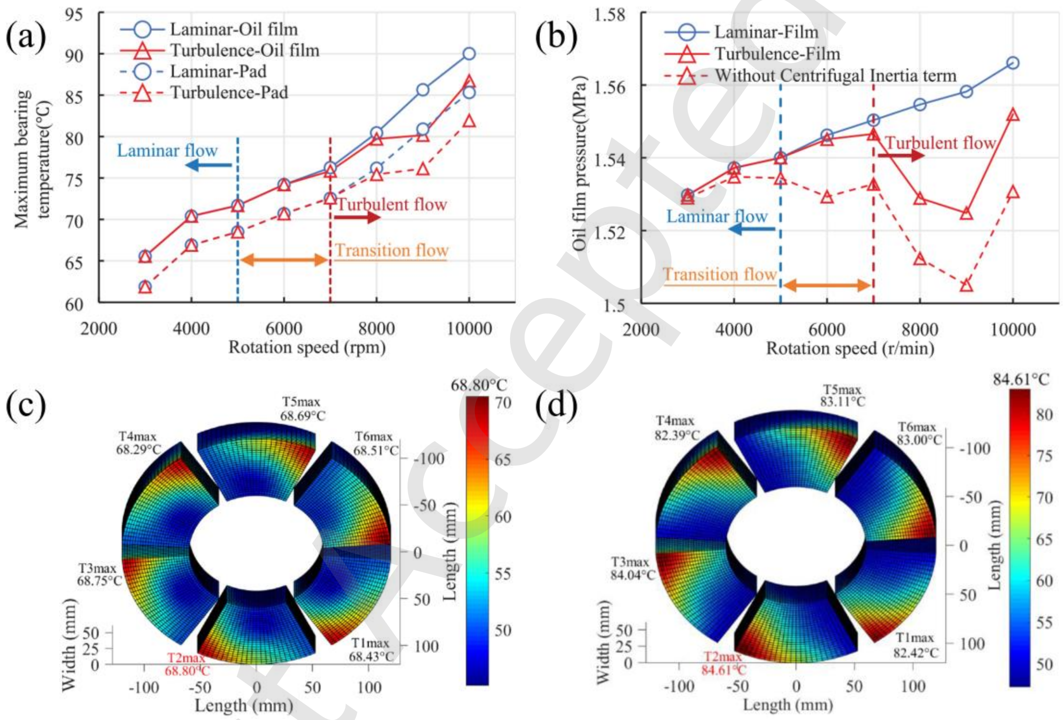

Fig. 4 The influence of turbulence model and misalignment on temperature and pressure characteristics of tilting pad thrust bearings (TPTBs)[42]. Influence of laminar and turbulent models on maximum bearing temperature (a) and on maximum oil film pressure (b) at different rotational speeds; temperature distribution of each pad under light load (c) and under heavy load (d) at a misalignment of 0.01° and rotational speed of 10,000 rpm.

TEHD theory evolved from THD theory, whose thermal-elastic deformation of the pad surface can be solved by methods such as the FDM, FEM, and simplified analytical method [43, 44]. Sternlicht [45] and Hashimoto [46] simplified the bearing pad into a 2D plate model and solved the thermal-elastic deformation of the pad surface via the thin plate deflection equation. Ashour et al. [47] obtained the pad deformation by solving the biharmonic bending equation under the thin plate assumption. These studies all adopted the two-dimensional adiabatic assumption, resulting in significant deviations between calculated results and measured data. Wang et al. [37] established a TEHD model considering the lubricant's viscosity-temperature effect and the elastic deformation of the pivoted pad, analyzed the oil film pressure using a 2D model, calculated the oil film temperature and bearing pad temperature respectively according to the 3D energy equation, and investigated the steady-state and dynamic characteristics of the pivoted thrust bearing combined with experimental tests.

In modern TEHD analyses of thrust bearings, more influencing factors have been incorporated to better align with actual operating conditions. Liu et al. [42] developed a TEHD analysis model for TPTBs that incorporates a turbulence model and centrifugal inertia terms, and the computational accuracy of the model was validated against ANSYS software. The results indicate that the TEHD model predicts the transition of oil film flow regimes more accurately than the THD model, highlighting the crucial role of deformation in calculating the Reynolds number and determining the laminar-to-turbulent transition. Turbulent flow can weaken the fluid shear effect and reduce the oil film temperature; the centrifugal inertia term affects the Reynolds number and pad temperature, while significantly increasing the maximum oil film pressure. Shaft misalignment leads to uneven temperature distribution and local overheating of the pads, an effect that becomes more pronounced under heavy load conditions. Relevant results are shown in **Fig. 4**. It is particularly noteworthy that, under transition and turbulent flow conditions, the erroneous application of a laminar flow model for calculation can lead to significant deviations in temperature prediction (with errors up to 50°C) [48]. Therefore, the corresponding model should be strictly selected based on the actual flow regime in the analysis. Koosha et al. [49] integrated the thermal mixing model of the feed groove and the flow starvation model into the TEHD analysis to investigate the effect of reduced oil supply flow rate on TPTB performance (relevant models are shown in Fig. 5). The results indicate that although reducing the flow rate can decrease drag power loss, it induces lubricant starvation, leading to a significant reduction in the minimum film thickness, as well as a sharp increase in the temperatures of both the oil film and pads, and exacerbated thermal deformation. This reveals that the oil supply flow rate is also a key factor that must be focused on in the TEHD analysis of thrust bearings.

Table 1 The relevant summary of the TEHD analysis of thrust bearings (a, b and c represent the FDM, FEM, and boundary element method, respectively.)

Ref.	Operating parameters		Model characteristics	Solution methods*			Conclusions	experimental comparison	Error
	n (rpm)	Load		a	b	c			
[37]	1,000–3,000	10–20 kN	» 3D TEHD model » Taking into the across-film viscosity-temperature effect	√	√		» The TEHD model achieves more accurate temperature calculations; » Axial stiffness and damping coefficients decrease with decreasing rotational speed and increase with increasing load.	√	Temperature error < 10%, stiffness variation < 20%, damping variation < 20%.
[42]	3,000–10,000	20 kN	» 3D TEHD » Taking into account shaft misalignment, turbulence, and centrifugal inertial terms	√	√		» Thermoelastic deformation affects flow regime prediction; turbulence reduces oil film temperature; centrifugal inertial terms increase oil film pressure; shaft misalignment causes local overheating.		
[48]	4,000–13,000	0.69–3.44 MPa	» 3D TEHD » Taking into turbulence and across-film viscosity		√		» Hard polymer pads exhibit large film thickness and low power consumption under turbulent flow, yet require a high supply flowrate; » Thick hard polymer liners have large deformation under heavy load	√	Temperature error < 10%.
[41]	100	4.9 MPa	» 2D TEHD	√		√	» The maximum pressure of the pad should be close to the pivot; » Large-scale bearings exhibit size effect.		
[40]	600	48 kN	» 2D TEHD	√			» Elastic deformation reduces the oil film hydrodynamic effect; » Thermal deformation enhances the hydrodynamic effect.		
[50]	2–10	900–1,500 kN	» 2D TEHD	√			» Radial/circumferential eccentricity, rotational speed, and load significantly affect lubrication performance.		
[51]	1,500–3,000	0.5–2.0 MPa	» 3D TEHD	√		√	» 3D TEHD model provide good predictions of bearing performance for both mineral and synthetic oils; » Replacing mineral oil with synthetic oil can enhance bearing efficiency and improve bearing safety.	√	Significant deviation in power loss; good agreement for other parameters.

*: The solution methods only include those explicitly mentioned in the references.

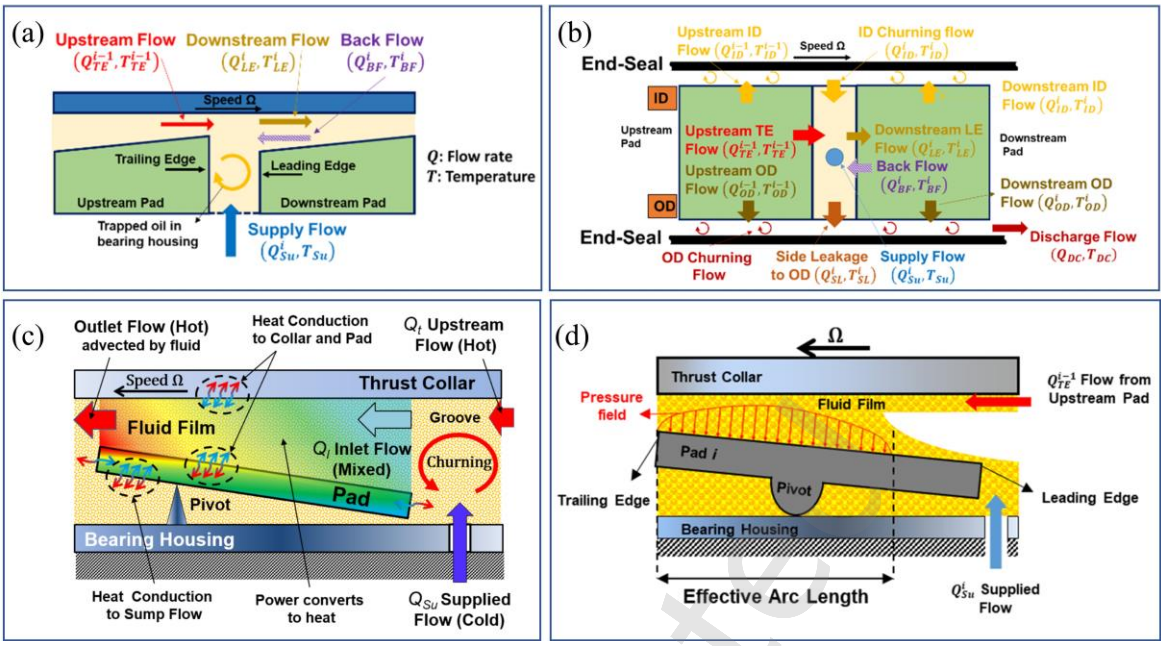

Fig. 5 Front view (a) and top view (b) of flow in the lubricant feed grooves of a TPTB with end seals [49]; (c) Schematic of fluid thermal mixing, flow in the feed groove, and heat transfer to bearing components [48]; (d) Idealized view of flow starvation in TPTB pad [49].

The development of THD and TEHD models has enabled accurate prediction of bearing temperature fields and oil film characteristics. However, the accuracy of these models is largely dependent on the reasonable definition of CHTC. Due to the precision limitations of the models themselves, 2D THD models only consider temperature gradients in the film thickness direction and ignore radial/circumferential heat conduction; thus, the CHTC has no significant impact on bearing performance [52]. In contrast, 3D THD models account for 3D temperature distributions and differences in local CHTC, so the CHTC has a significant effect on the temperature rise on sliding surfaces [30]. The assumed CHTCs in T(E)HD analysis of thrust bearings across different studies are shown in **Table 2**.

In early theoretical analyses of thrust bearings, the CHTC was commonly assumed as a global constant based on engineering experience and adjusted according to pad size[53, 54]. However, studies have shown that the distribution of CHTC across different locations on the thrust pad is significantly non-uniform and influenced by multiple factors. Based on experimental measurements and regression analysis of seven thrust bearings of different sizes, Ettles et al. [55] proposed an empirical CHTC formula for specific tilting-pad thrust bearings, indicating that the CHTC at the outer radial surface is approximately four times that at the back surface, while the coefficients at the leading edge, trailing edge, and inner radial surface are about twice that of the back surface. Although useful for preliminary assessment of similar bearings, this relationship represents a qualitative average derived from tests on a specific bearing geometry. In practice, its applicability may be limited due to variations in support type, surface condition, and flow distribution. By comparing theoretical and experimental results, Markin et al. [56] identified optimal CHTC values of 100 W/m²·K for the main surface and 500 W/m²·K for the outer trailing edge of thrust pads with spherical or spring supports. Wodtke et al. [57] further emphasized that different forms of CHTC notably affect the temperature distribution of the pad. They demonstrated that h_c var yields better agreement with measured temperature fields in TEHD predictions, whereas h_c const provides closer predictions of oil film thickness.

In summary, the determination of CHTC is crucial for accurately predicting the performance of thrust bearings. Its value is subject to the complex coupling effects of bearing structure (e.g., dimensions, support type, oil cavity design), operating conditions (e.g., rotational speed, flow regime), and heat transfer surface location, exhibiting significant non-uniformity. Consequently, the simplistic assumption of a global constant for CHTC should be abandoned in favor of a case-specific determination based on the relevant parameters. Existing research data with similar geometries and operating conditions in **Table 2** can be referenced as initial estimation values, but close attention must be paid to their application boundaries. Furthermore, it is recommended that theoretically selected CHTC values be validated and calibrated through scaled model tests or prototype measurements to ensure predictive accuracy.

Table 2 The assumed CHTCs in T(E)HD analysis of thrust bearings across different studies

Ref.	Bearing pad dimensions		CHTC (W/m²·K)	Notes
	Outer diameter (m)	Iner diameter (m)		
[53]	0.5		567	Empirical value
[54]	0.65–3.1		567	When the outer diameter of the pad exceeds 0.76 m, the coefficient shall be adjusted to 280–425 W/m²·K.
[56]	0.22	0.12	H=100, H_c=500	Through parameter tuning, the optimal value of the coefficient is determined.
	0.96	0.62		
[57]	5.2	3.25	h_c const=750; h_c var: 20-420	Based on calculations using FSI technology, the coefficients on different bearing pad surfaces vary.
[55]	0.15-2.95	0.08-1.5	$F = 25.5U^{0.7}\eta_{ch}^{-0.2}B^{-0.4}$	The support types of thrust bearings include point support and line support, and their materials are steel or cast iron.
[58]	2.2	1.05	Values are determined with reference to the studies by [55] and [54].	
[59]	2.94	1.5	450	The surface CHTC is inferred from temperature measurement data.
	0.78	0.42	$-162+16.2\omega$, for $\omega > 10$ rad/s	From measured data, the correlation between the surface CHTC and rotational speed is established, and the empirical formula is derived.

	0.15	0.08	Oil-contacting surfaces are set to 1000; oil-free areas are set to 10.	Consider the effect of the support structure on CHTC.
[49]	0.27	0.13	100–450	Values are determined with reference to the studies by [55] and[59].

2.3 Lubrication characteristics analysis based on CFD

As the core models of fluid lubrication theory, both the classical Reynolds equation and generalized Reynolds equation are based on the Navier-Stokes equation and employed to solve the lubrication characteristics of thrust bearings. Specifically, the classical Reynolds equation is a simplified model derived from assumptions of constant viscosity, laminar flow, and neglect of inertial forces and curvature effects, which is suitable for analyzing basic operating conditions. By contrast, the generalized Reynolds equation incorporates conditions such as the viscosity-temperature effect, turbulence correction factors, and mass conservation boundaries, thus being applicable to complex operating conditions. However, the generalized model still ignores the variation in oil film curvature and relies on averaging assumptions, making it incapable of analyzing the flow characteristics of local features (e.g., oil grooves and chamfers). Moreover, it adopts a decoupled iterative method to tackle TEHD multi-physics coupling, leading to computational errors under complex operating conditions. With the development of computational technology, solving the Navier-Stokes equation by combining CFD analysis software and solid finite element analysis software to analyze the lubrication characteristics of thrust bearings has emerged as an effective approach to resolving the aforementioned issues.

2.3.1 CFD modeling method

The CFD modeling of thrust bearings encompasses 2D and 3D models. Although the efficient computation of 2D CFD simulations is realized by simplifying geometric and boundary conditions, 2D models are not capable of reflecting curvature effects, real geometric features, 3D heat conduction characteristics, and complex elastic deformations. Their accuracy decreases significantly under complex operating conditions such as shaft misalignment and non-uniform loads, thus being only suitable for parametric analysis in the preliminary design stage or performance evaluation under symmetric operating conditions. In contrast, 3D models provide more reliable theoretical support for performance prediction and structural optimization under complex operating conditions. In early studies, Rotta et al. [60] first evaluated the applicability of ANSYS software in analyzing bearing flow phenomena through a simple 2D model with fixed-geometry sliding blocks. Subsequently, the clearance between bearing pads was further incorporated into the model [61]. Since centrifugal force acts on the lubricating oil between gaskets, the radial component of velocity is of great importance. Therefore, the research team [62] further employed a 3D model to analyze the lubricant fluidity and cooling performance under different oil supply methods.

In CFD simulation studies of thrust bearing lubrication performance, the 3D modeling approaches exhibit a progressive characteristic from localized to global models. For investigating localized flow characteristics in complex structures, such as the influence of surface textures on lubrication performance, researchers often adopt simplified local models to avoid the excessive computational burden associated with full models. As shown in Fig. 6(b), a local CFD model established for straight-groove textures takes cavitation effects into account while neglecting factors such as thermal deformation, with a focus on studying the influence of Reynolds number, depth ratio, and area ratio on the internal flow behavior within the textures[63].

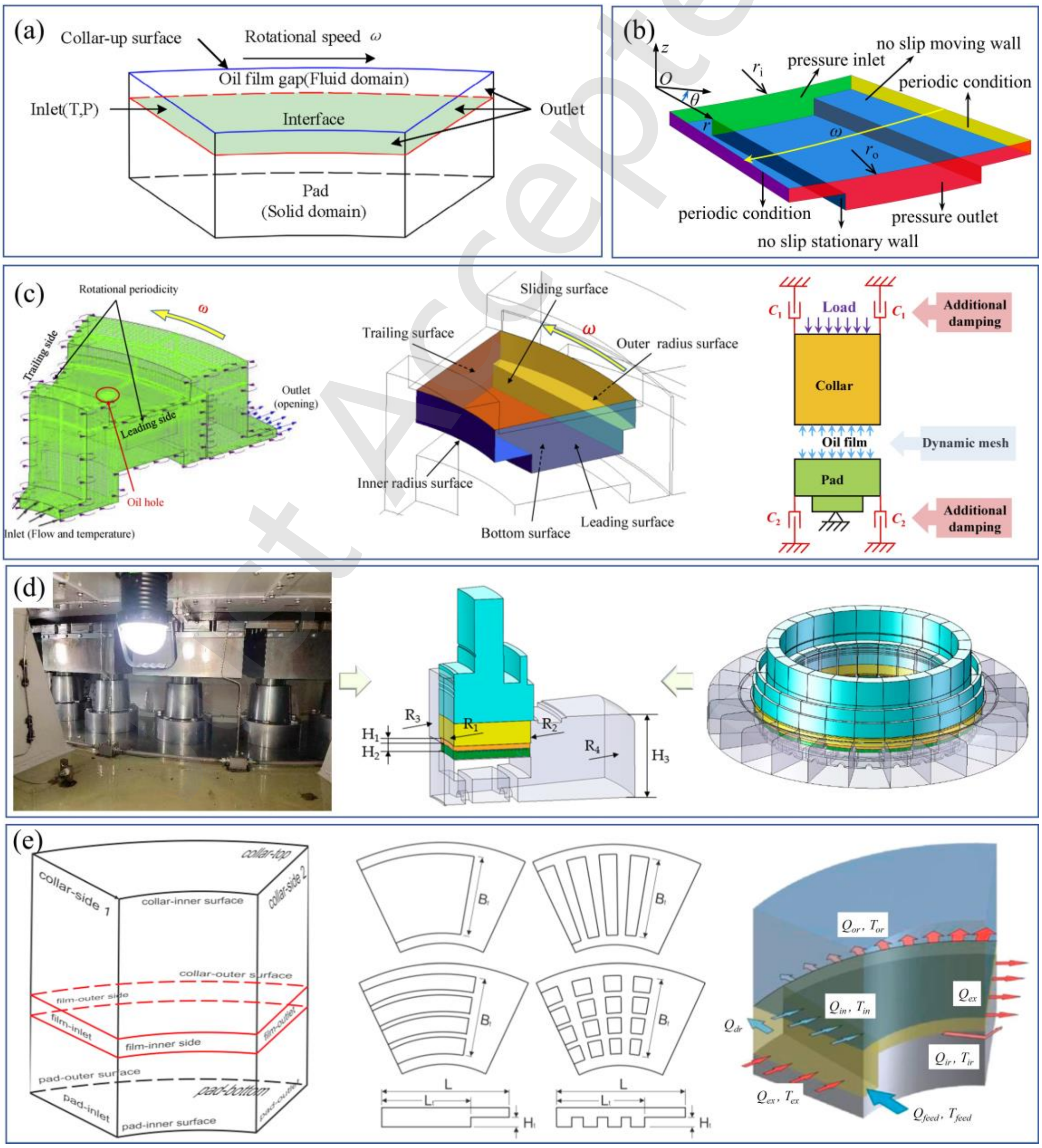

Fig. 6 CFD modeling method. (a) 3D model of pad and boundary conditions [64]; (b) Local model of a single groove and boundary conditions [63]; (c) Cyclically symmetric model with oil holes and principle of additional damping for delayed motion [65]; (d) Physical pictures and model diagrams of the thrust bearing of the hydro turbine unit in Hydropower Station [66]; (e) Schematic of boundary conditions, textured structure, and lubricant mass flow rate for the integral model of textured thrust sliding bearing [67].

To accurately simulate the lubrication characteristics of thrust bearings under actual operating conditions, it is necessary to develop complex models that account for multiphysics coupling effects. The computational domain in these models typically encompasses a single pad, the corresponding collar section, and the intervening lubricant film. The collar structure may be omitted if interactions between the collar and the pad or lubricant are not considered. By preserving the key structural features of thrust bearings while effectively balancing computational cost and simulation accuracy, this approach has become a widely adopted simplified modeling methodology in research. Fig. 6(e) illustrates a model constructed using this approach, whose advantage lies in its simultaneous consideration of the pressure and temperature fields within the lubricant domain during heat dissipation, as well as the temperature fields of the pad and collar during conjugate heat transfer[67]. However, due to the large number of textures in the computational domain, cavitation effects are generally not considered in such models. Li et al. [64]established a 3D fluid lubrication model for thrust bearings using CFD and FSI techniques, proposing a mesh motion algorithm based on a User-Defined Function (UDF) suitable for dynamic grid updates in transient numerical simulations. The model and its boundary conditions are presented in Fig. 6(a). Cao et al. [65] employed a fluid-solid-thermal interaction method to simulate the lubrication characteristics of thrust bearings during the start-up and shutdown processes of pumped storage units, establishing a cyclically symmetric model incorporating oil holes. Considering the difficulty of generating sufficient hydrodynamic pressure to balance the external load during the initial stage, additional damping was introduced into the pad and collar to delay motion, thereby ensuring automatic iterative convergence of the oil film thickness. Fig. 6(c) illustrates this model and the working principle of the additional damping for motion retardation.

To comprehensively evaluate the performance of thrust bearings within a complete lubrication system, it is essential to construct a full-system model that integrates the shaft, thrust pads, collar, oil tank, and support components (Fig. 6(d)) [66]. To balance computational efficacy and accuracy, two strategies are commonly employed: 1) assuming uniform load distribution to construct a cyclically symmetric model [68]; 2) implementing domain-divided meshing for the oil film region and oil tank region, and conducting local mesh refinement for key regions [69], so as to adapt to the differences in complex geometric scales.

2.3.2 T(E)HD analysis based on CFD

The study on the thermal effect of thrust bearing oil film is a complex field involving multiple factors [12]. Thrust bearings usually operate under high-load and high-speed conditions. During operation, heat is generated by viscous shear in the lubricant and friction between the rotating collar and pad, which may lead to a decrease in lubricating oil viscosity, bearing surface deformation, and increased wear [70-73], thereby significantly affecting the overall lubrication performance of thrust bearings.

Traditional TEHD methods require assuming the CHTC during solution (Section 2.2). However, a significant advantage of the thermal-fluid-solid interaction technology based on CFD is that it does not need to assume the CHTC at the fluid-solid coupling interface. Instead, this coefficient is obtained during CFD calculations and automatically updated at each iteration step, ensuring the calculation accuracy of T(E)HD analysis for thrust sliding bearings. Grzegorz et al. [74] conducted 3D calculations using CFD to analyze the lubricating oil flow in the oil supply system of the leading edge groove of hydrodynamic thrust pads. The model considered the SST turbulence model and assumed adiabatic boundary conditions for the pads and thrust collar, or isothermal boundary conditions. Pu et al. [75] established a 3D model of thrust bearings with circular defects. The model employed CFD dynamic mesh to handle oil film region changes caused by pad oscillation and thrust collar movement, and combined with the thermal-fluid-solid interaction technology, enabling the accurate calculation of pad inclination angle, thrust collar displacement, and lubrication characteristic parameters when the oil film force balances the external load. The calculation flow chart based on the CFD dynamic mesh method is shown in **Fig. 7**. Zoupas et al. [76] conducted a CFD-based THD study on the influence of manufacturing defects on the performance of large tilting-pad thrust bearings, finding that under normal bearing loads, defects mainly affect the minimum oil film thickness, while under heavy loads, defects have a greater impact on the maximum oil film pressure.

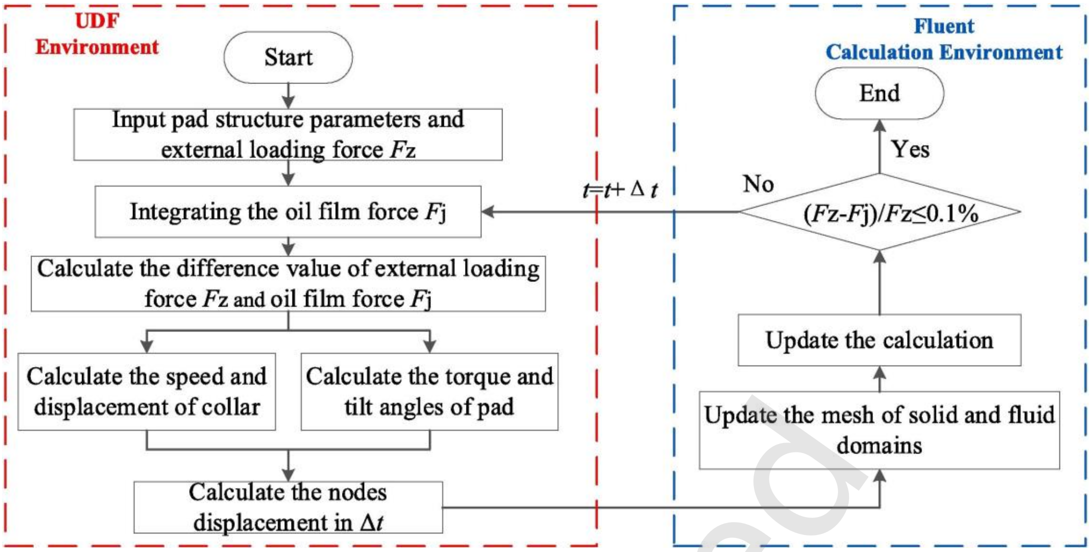

Fig. 7 The calculation flow chart based on CFD dynamic mesh method

None of the aforementioned studies considers the thermoelastic deformation of bearing pads or thrust heads. Pajączkowski et al. [39, 77] conducted 3D TEHD analysis on tilting-pad thrust bearings of large hydraulic turbines to study their steady-state and transient lubrication performances. This method analyzed the oil tank region with oil film via CFD, and calculated the thermoelastic deformation of thrust pads and thrust collar in ANSYS; the two were connected through fluid-solid coupling, forming a bidirectional feedback mechanism: the thermoelastic deformation of pads and thrust heads changes the geometric shape of the oil film gap, while the oil film pressure and heat flux act back on the structure as boundary conditions to calculate its thermoelastic deformation. Wodtke et al. [78, 79] validated the accuracy and limitations of both models by comparing the TEHD model based on the Reynolds equation and CFD simulation results with measured data from a large thrust bearing. The results showed that the CFD model predicted the pad temperature field and maximum oil film pressure more closely to the measured data, while the traditional TEHD model provided more accurate predictions of oil film thickness. Both models still exhibited discrepancies with the measurements in details such as pressure distribution, due to simplifications of the actual geometry and operating conditions. Zhai et al. [80] proposed a bidirectional coupled three-dimensional TEHD method combining CFD and finite element analysis (FEA) for the lubrication analysis of pump-turbine thrust bearings (as shown in **Fig. 8**). The computational accuracy was effectively improved through the combination of direct and partitioned coupling approaches. Comparative results indicated that the predicted pressure distribution on the pad surface agreed well with experimental data; the deviation between predicted and measured temperatures at key monitoring points was approximately 5%; and the error in predicted thrust load was only 0.75%. This research team further used this method to analyze the oil film pressure, temperature, thickness distribution of TPTBs, and the deformation of pads and thrust heads, revealing characteristics such as no pressure gradient but significant temperature gradient in the oil film thickness direction, and complex distribution of heat transfer coefficient on the pad surface [81]. Notably, traditional TEHD methods based on the Reynolds equation and FEA require defining the initial oil film thickness, radial and circumferential inclination angles, whereas this model only needs to define the initial oil film thickness. This is because the oil flow process forms high pressure at the inlet and low pressure at the outlet, thereby enabling the pads (or collar) to automatically generate radial and circumferential inclination angles.

In summary, the research on multi-physics coupling theory (**Fig. 9**) has become an indispensable tool for evaluating the performance of thrust bearings. Studies have developed from initial 2D models to complex 3D coupling models that can more accurately simulate actual operating conditions. During the analysis process, the influences of multi-physics factors, such as the elastic deformation, thermal deformation and their interaction of bearing pads and mirror plates, viscosity-temperature effect, turbulence, shaft misalignment, and oil supply conditions, have gradually been incorporated. To further reduce programming workload and improve calculation accuracy, researchers combined self-developed programs with commercial software, analyzed the thermoelastic deformation of bearing pads and mirror plates via ADINA or ANSYS finite element programs, and used these deformations as boundary conditions in their self-developed programs that solved the coupled Reynolds equation, viscosity-temperature equation, film thickness equation, and energy equation [82-85].

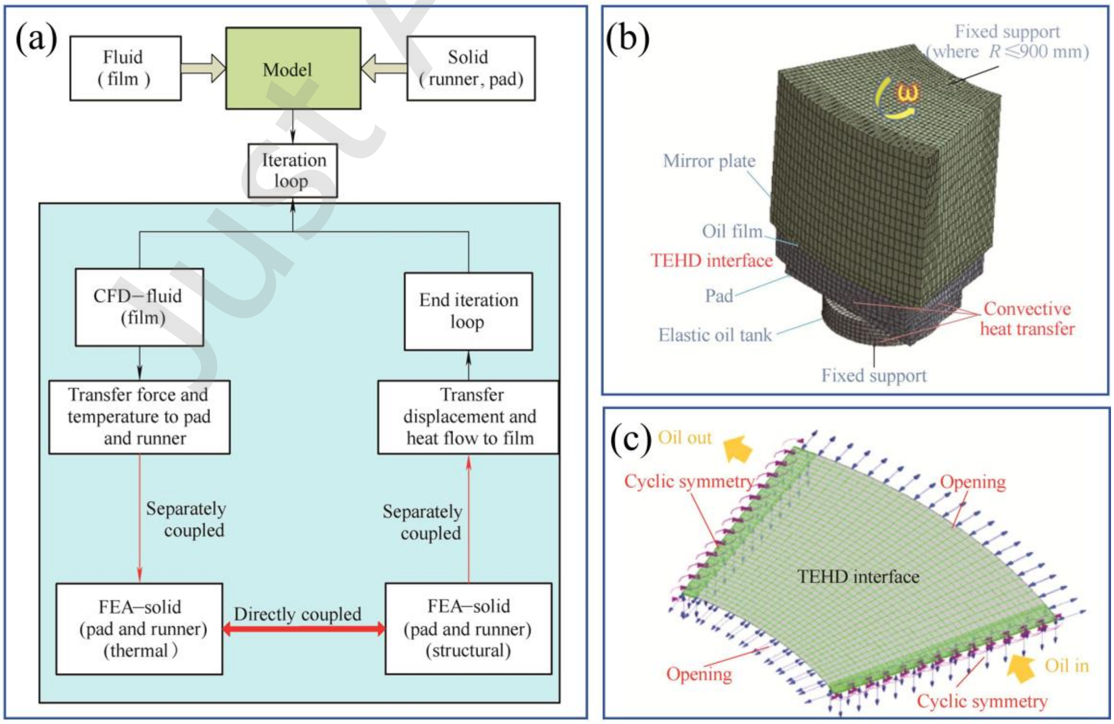

Fig. 8 (a) Iteration process for the TEHD lubrication two-way coupled solution; (b) Solid model for the pad and mirror plate; (c) Fluid model for oil film [80].

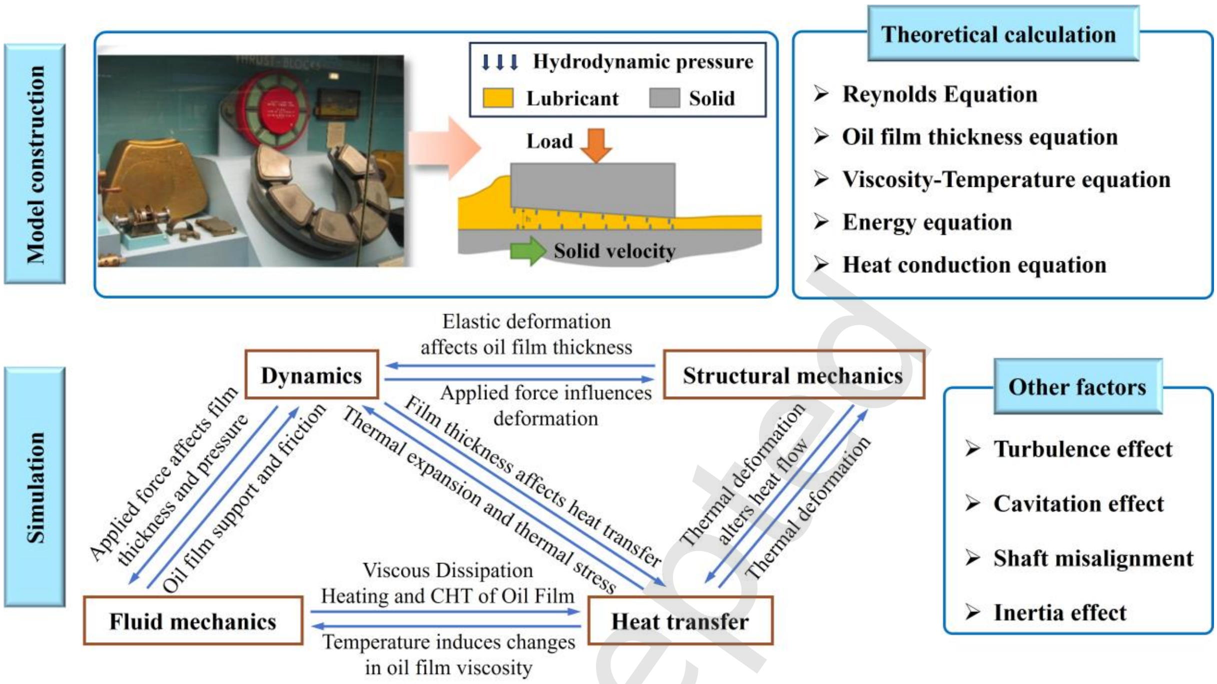

Fig. 9 Basic framework of research on multiphysics coupling theory

However, the establishment of models for transient processes, critical behaviors of thermal instability, and coupled dynamic effects in existing theories still requires further innovation and improvement. And theoretical model predictive reliability under complex operating conditions needs to be further verified with experimental data. Since the current experimental validation system remains incomplete, it is necessary to establish a standardized experimental benchmark platform for bearing performance or integrate operational data from actual units to build a comprehensive model calibration system. Based on this, this paper systematically reviews advances in experimental testing technologies for thrust bearings in Section 3, aiming to provide a systematic reference for the design and construction of subsequent experimental platforms.

3 Thrust bearing performance testing technologies

In the research field of thrust bearings, the combination of computational methodologies and experimental verification has emerged as a critical avenue for revealing their lubrication characteristics [86]. Numerical simulation and finite element analysis provide critical theoretical support for the precise prediction of lubrication characteristics and optimal design of thrust bearings. Although current research has established a framework of lubrication models and algorithms that encompass multi-physics coupling and can comprehensively account for multi-dimensional influencing factors such as complex operating conditions and material properties, the accurate assessment of their actual lubrication performance remains highly reliant on experimental testing and validation. Predictive data generated by numerical methods must be corrected and validated against experimental measurement results. Consequently, the establishment of an experimental analysis platform for the benchmark performance of thrust bearings has become an indispensable foundation for bridging numerical prediction and engineering applications.

3.1 Performance testing equipment for thrust bearings

According to differences in experimental objects and requirements, thrust bearing test devices can be classified into two types: basic tribological test devices and bearing model test devices.

3.1.1 Basic tribological test devices

For basic tribological property testing, research on thrust bearings focuses primarily on material modification [87], surface treatment [88], and structural characteristic optimization [89]. Testing modules of the relevant test benches encompass experimental test devices such as Block-on-Ring and Pin-on-Disc [90, 91], enabling different types of friction tests (e.g., rotational, reciprocating, and micro-motion tests) on specimens. These modules can either be custom-designed according to research requirements or utilize dedicated functional components from universal friction and wear testing machines like UMT and SRV. Related studies typically employ friction coefficient (COF) and wear volume as key measurement metrics to conduct comparative analyses of different bearing materials and structural features. Furthermore, through characterization techniques such as Scanning Electron Microscopy (SEM), Atomic Force Microscopy (AFM), and X-ray Diffraction (XRD), the surface morphology, elemental distribution, and compositional content of specimens can be analyzed. Thereby revealing fundamental tribological behavior mechanisms including material wear states [92] and stick-slip phenomena [93]. Li et al. [94] have established a numerical model for optimizing the surface texture distribution of thrust bearings based on the GA-SQP hybrid algorithm. They have carried out multi-condition experiments using a Plint TE92 friction and wear tester to experimentally verify the numerical optimization model, thereby achieving the organic integration of theoretical research and experimental testing. Lan et al. [95] have investigated the abrasive wear performance of aromatic thermosetting polyester-based coatings (ATSP) and polyether ether ketone-based coatings (PEEK) using an ultra-high-pressure pin-on-disc friction and wear tester. The experimental variables include test duration, different silica sand particle sizes, and different pin materials, and they have verified the wear mechanism of ATSP using SEM and XPS.

3.1.2 Thrust bearing model test devices

Thrust bearing model test devices evaluate the overall lubrication performance of thrust bearings by detecting core lubrication parameters such as oil film thickness, oil film pressure, and oil film temperature under different operating conditions. Typical test benches typically consist of five basic modules: loading system, experimental test main body, cooling and oil supply system, detection and control system, and drive system. Based on the principle of structural similarity, thrust bearing test benches can be classified into two types: scaled-down models and full-scale models; by structural form, they are categorized into vertical and horizontal types. The construction of test benches must combine research objectives and structural characteristics of industrial shafting systems: vertical test benches are widely used in vertical shafting systems such as hydroelectric generating units and nuclear main pump thrust bearings; horizontal test benches are adapted to horizontal shafting systems such as marine propulsion systems and heavy-duty gas turbines.

Table 3 lists the functional characteristics of representative thrust bearing test benches, with the test bench structures of some typical studies shown in **Fig. 10**. In the 1990s, the Institut Pprime (France) designed and developed a vertical thrust bearing test device, which has been modified several times to incorporate new measurement technologies and lubrication modes; its latest thrust bearing test bench is shown in **Fig. 10(b)**. The research team has conducted extensive studies on various types of bearings, including TPTBs and fixed-geometry thrust bearings. Using the initial thrust bearing test bench, Dadouche et al. [72, 73] from this team have investigated the lubrication characteristics of fixed-geometry thrust bearings under different operating conditions, and verified the results against simulation data. Subsequently, Harika et al. [96] changed the mechanical loading to pneumatic jack loading and introduced spherical hydrostatic bearings to eliminate static misalignment, and then used the upgraded test bench to investigate the influence of water contamination in oil on the performance of TPTBs. Later, Henry et al. [97-99] successively conducted in-depth studies on the hydrodynamic behavior of conical stepped thrust bearings, the lubrication performance of textured thrust bearings, and their lifting capacity during start-stop phases, and compared these with traditionally designed bearings. Regarding the issue that thrust bearings have limited load capacity at low sliding speeds and that contact with sliding surfaces during start-stop phases results in severe wear, Bouyer et al. [100] used this test bench to conduct experimental studies on the lubrication performance of a flat land thrust bearing with pockets under three lubrication modes: hydrodynamic, hydrostatic, and hybrid lubrication.

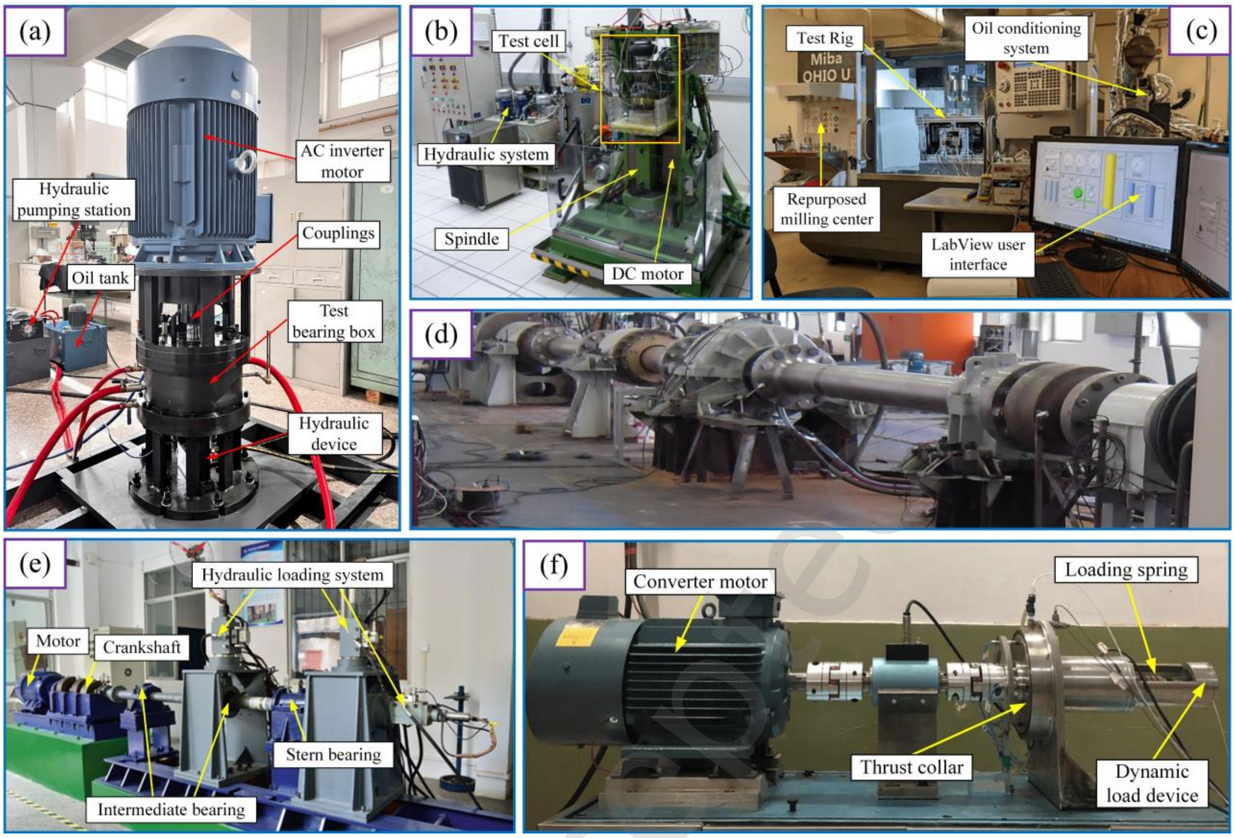

Fig. 10 Typical sructure of trust siding baring test Bench. (a) Scaled-down Test Rig for Thrust Bearing of Nuclear Main Pump[101]; (b) The vertical thrust bearing test device designed and built by Pprime Institute [100]; (c) Test platform for thrust sliding bearings retrofitted from existing mechanical equipment [102]; (d) Full-scale Propulsion Shafting Test Bench [103]; (e) and (f) Comprehensive Performance Test Platform for Marine Shafting [104, 105].

Though most lab-scale test rigs are composed of custom-designed components and assemblies, retrofitting existing machinery into the main body and driving device of test rigs offers considerable practical utility. Based on the vertical thrust bearing test rig designed by Myers et al. [106], researchers from Ohio University (USA) retrofitted milling machines and lathes into the main body and drive system of the test rig. This platform was successfully applied to thrust bearing experiments, with its latest configuration shown in **Fig. 10(c)**. Through iterative design of the experimental platform, the team continuously refined the bearing alignment system to guarantee precise alignment between the bearing and rotating parts. Currently, the team has fabricated a variety of bearing samples with fixed geometric structures, explored the influence of taper depth on operational parameters (e.g., temperature, pressure distribution) under different combinations of rotational speed, load, and oil supply temperature, and compared the experimental findings with those obtained from numerical simulations [102, 107, 108].

During the actual operation of thrust bearing systems for heavy/large-scale equipment, the bearing lubrication performance is degraded due to complex operating conditions, thus impairing the safety of the overall system.

Therefore, considering practical requirements, the experimental research on the thrust bearing shafting systems of heavy/large-scale equipment typically encompasses multiple aspects. Li et al. [109] designed and constructed a scaled vertical thrust bearing test rig system for the nuclear main pump, to simulate the actual working state of the thrust bearing, whose main structure is shown in **Fig. 10(a)**. To explore the feasibility of the pad scaling scheme and meet the test rig's safety requirements, the team compared the test rig's rotational speed and load with those of the actual unit at different ratios, and verified the comparison via simulations. Subsequently, Pu et al. [75] and Xie et al. [101] used this test rig to investigate the effects of pad surface defects and scratch structural parameters on the lubrication characteristics of the thrust bearing. Wang et al. [110] designed and constructed a vertical multi-functional test rig for performance testing of thrust bearings in nuclear main pumps. Besides satisfying basic loading tests, this test rig also enables the conduction of tests on bearing oil film thickness, friction coefficient, and simulated coast-down tests. Currently, this test rig has been used to conduct durability operation tests in a localization project of large-thrust bearings for a nuclear main pump. In addition to the overall design of test rigs, some scholars have optimized the design of key components of nuclear main pump thrust bearing systems (including support structures, cooling and lubrication devices, and lubricating oil circuits), aiming to address the performance deficiencies of traditional test rigs [111-114].

Table 3 Functional characteristics of different thrust bearing test rigs

Types	Applications of the test rigs	Composition of the test rigs		Experimental test parameters	Ref.
		Driving module	Loading system		
Vertical thrust bearing test rigs	1. Evaluate the performance of bearings with different taper depths. 2. Analyze the effects of spiral cone angle, etc on key performance parameters	The Haas VF-1 vertical CNC milling machine, spindle max speed: 15,000 rpm.	Spring force thrust loading system	» Taper depth: 0.0005″ -0.0025″ » Load: 0.45–2.2 kN » Rotational speed: 1,500–6,000 rpm.	[102]
	1. The transient behavior of bearings during start-up/ shutdown. 2. Provide experimental data for optimizing nuclear main pump thrust bearing designs.	90 kW AC motor, regulated by a frequency converter with a maximum speed ≤ 3,000 rpm.	Hydraulic pump	» Rotational speed: 1,485 rpm » Load: 15.1 kN » Lubricant temperature: 60℃	[109]
	1. Validate wear models and CFD simulations for TPTBs. 2. Investigate the influence of scratch structural parameters.			» Rotational speed: 500–1,485 rpm » Load: 5–16.7 kN » Lubricant temperature: 60℃	[101]
	1. Investigate the performance of thrust bearings under different lubrication modes. 2. Analyze the characteristics of steady-state and transient startup/shutdown conditions.	Driven by a 15 kW DC motor, speed range 0–10,000 rpm.	Pneumatic jack	» Rotational speed: 0–8,000 rpm » Load: 0.5-2.5 kN	[100]
	1. Study on the static and dynamic characteristics of tilting-pad thrust bearings. 2. Suitable for axial vibration research of turbomachinery.	Motor drives the main shaft via flexible coupling with a speed controller.	» Stepper motor drives ball screw » Electromagnetic exciter.	» Rotational speed: 0–3000 rpm » Static load: 0–7 kN » Dynamic load: 0.027 kN	[115]
	1. Investigating the influence of various variable parameters on oil film thickness. 2. Validating the effectiveness of ultrasonic measurement methods	The motor adjusts the rotational speed via belt drive.	Hydraulic loading system	» Rotational speed: 400、800、1,200、1,800 rpm » Load: 2.45–8.25 kN	[116]
	1. Validation of transient model accuracy. 2. Study of performance changes during startup and shutdown	The motor drives the main shaft to rotate		» Rotational speed: 0–200 rpm » Load: 0.1 kN	[117]

Horizontal thrust bearing test rigs	1. Study the performance of TPTBs during the transition to mixed friction. 2. Test bearing material properties and validate feasibility under extreme conditions.	Motor drives the main shaft via a frequency converter for speed control.	» Hydraulic piston loading system » Maximum load: 90 kN	» Rotational speed: 0–4,500 rpm » Load: 10–90 kN	[118]
	For the study of tribological and vibration performance of different types of thrust bearings.	Variable-frequency motor drives the main shaft to rotate.	» Spring-screw loading device » Maximum load: 10 kN	» Rotational speed: 100–600 rpm » Specific pressure: 0.1–0.5 MPa	[104]
	1. Measure oil film stiffness and damping under various operating conditions 2. Vibration characteristics of the shaft system		Hydrostatic thrust bearing for loading	» Rotational speed: 70–800 rpm » Load: 30–44 kN » Impulse hammer for transient excitation	[32]
	1. Load carrying capacity of tilting-pad thrust bearings 2. Investigation of lubrication state transitions	The servo motor drives the main shaft via a coupling	Pneumatic loading	» Rotational speed: 600–1,600 rpm » Specific pressure: 0.1–0.6 MPa	[119]
	Static and dynamic characteristics test	The motor drives the main shaft through a gearbox.	High-pressure oil for static loading	» Rotational speed: 1,000–3,000 rpm » Load: 10–20 kN	[37]

The propulsion shafting system of a ship is generally composed of structures such as propellers, stern shafts, intermediate shafts, couplings, coupling flanges, radial support bearings, and axial support bearings, and is rotationally driven by the main engine or the main engine output gear reducer[120]. The design and construction of its test rig system are basically consistent with the actual ship propulsion shafting system. Due to the large size and space occupation of the propulsion shafting systems of large and medium-sized ships, full-scale shafting test rigs for such ships are mostly constructed in ship research institutes or military units. For example, the China Ship Development and Design Center [103, 121] constructed a full-scale propulsion shafting test rig with a full length of tens of meters, as shown in **Fig. 10(d)**. For medium and small-scale scaled-down shafting test rigs, scholars from Wuhan University of Technology [104, 105, 122] designed a comprehensive test platform for ship shafting performance, which is used for researching and verifying shafting alignment methods, bearing loads, shaft segment deflection, stress changes, and vibration characteristics of different installation forms (**Figs. 10(e) and (f)**).

Experimental research on thrust bearings of hydropower units generally adopts large-scale thrust bearing test platforms. For instance, Dongfang Electric Corporation (DEC) designed and constructed a 1:1 full-scale thrust bearing test platform for large hydropower turbines, whose inner and outer diameters of the thrust disk are 1,300 mm and 2,400 mm respectively. Subsequently, thrust bearing bushing temperature experiments and oil film thickness measurement experiments were conducted on this platform, providing an experimental basis for the practical application of large thrust bearings [123, 124]. Jia [125] used a 2,000t high-speed heavy-load bidirectional thrust bearing test rig to measure data including thrust pad temperature, oil film thickness, and oil film pressure, and compared the measured data with calculation results, verifying the correctness of the bearing design and calculation.

3.2 Monitoring methods for performance parameters of thrust bearings

To investigate the lubrication performance of thrust bearings, it is necessary to acquire the basic performance parameters of the bearings. During the actual operation of the bearings, relevant parameters also need to be continuously monitored to promptly detect and address potential fault risks. The core monitoring parameters for the lubrication of thrust bearings include oil film pressure, oil film thickness, and temperature. Therefore, this section summarizes their different testing methods and technical characteristics, as shown in **Fig. 11**.

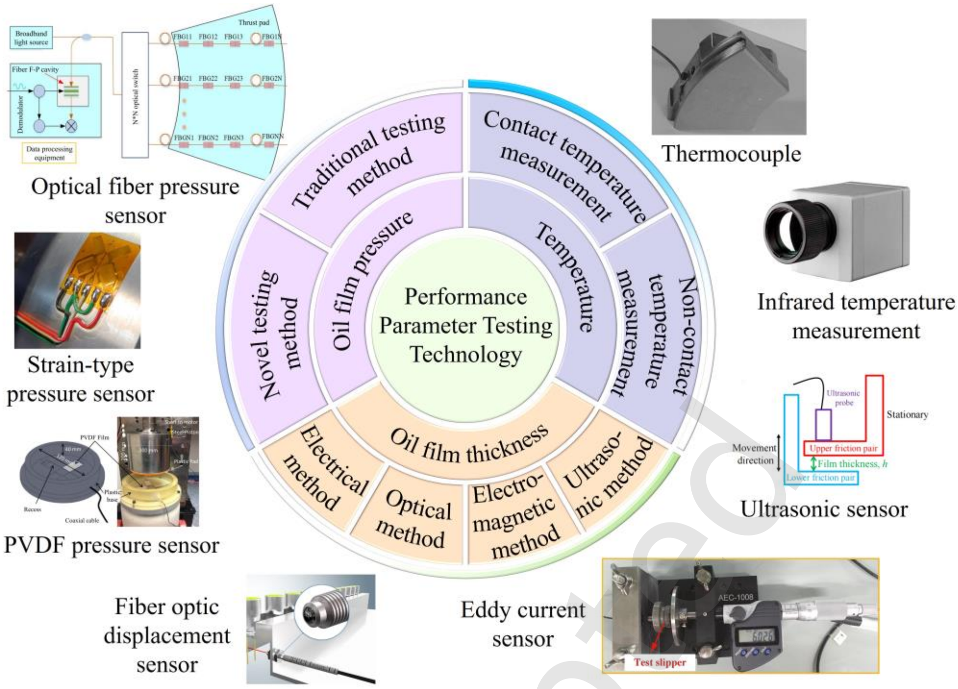

Fig. 11 Testing technology for performance parameters of hydrodynamic thrust bearings.

For oil film pressure measurement, traditional strain gauge pressure sensors or piezoelectric pressure sensors are typically used [100, 109]. With the development of sensing technology, MEMS-based silicon piezoresistive pressure (SPP) sensors [126, 127] and fiber Bragg grating (FBG) sensors [128] have begun to be applied in oil film pressure monitoring; these sensors can be installed on bearing bushings or shafts to enable pressure monitoring at fixed points. In contrast, arrays of new piezoelectric materials (e.g., PVDF or EMFi) [129] can cover the full bearing pressure distribution, but their technical maturity and installation complexity are relatively high. It should be noted that the layout of measurement points and sensor installation may disrupt the lubricating state of the bearing working surface and cause significant measurement errors. Additionally, the dynamic monitoring of new sensors lacks analysis based on relevant theoretical models; both aspects require balancing measurement accuracy and engineering applicability.

Temperature monitoring methods are classified into two types: contact-type and non-contact-type. Contact temperature measurement methods are mainly implemented via sensors such as thermocouples and FBG sensors to directly measure temperature variations at different positions, featuring high accuracy and mature technical maturity [118, 130, 131]. Infrared temperature measurement technology [132, 133] can achieve non-intrusive temperature monitoring with an accuracy of up to 0.1°C; however, strict emissivity calibration of the measured object is required, and the measurement accuracy is susceptible to interference from ambient temperature. Overall, contact temperature measurement technology has mature technical performance and low cost, but it is also prone to limitations from installation positions and may interfere with the flow field. Non-contact technology shows greater potential in dynamic temperature field analysis but is restricted by environmental factors.

Existing oil film thickness measurement methods mainly include electrical methods, optical methods, electromagnetic methods, and ultrasonic methods. Optical methods [134-136], which include techniques such as light interference and optical fiber displacement, feature high resolution and high accuracy, and enable direct observation of lubricating film distribution; however, they require an optical path inside the friction pair. Electrical methods based on resistance [137] and capacitance [138] principles are susceptible to noise and electromagnetic interference during monitoring. Eddy current sensors [139] are widely used due to advantages such as good stability, fast dynamic response, and a wide measurement range, but they are only applicable to conductive materials. Although electromagnetic methods [140] have high measurement accuracy, they are intrusive to rotating components. Compared with the aforementioned methods, the ultrasonic method is a non-destructive testing method that does not damage the structure and flow field of the lubricating oil film, and does not require light transmission or insulation conditions. Thus, it is often used for film thickness measurement of rotating components under actual operating conditions. The ultrasonic methods for film thickness measurement include time-domain methods and frequency-domain methods. Time-domain methods (e.g., the time-of-flight model [141], time-frequency analysis method [142], and unified time-domain model [143]) calculate film thickness based on the time interval of reflected waves. However, when the film thickness is small, the time interval is difficult to distinguish due to overlapping wave peaks. Frequency-domain methods, on the other hand, extract the amplitude-frequency characteristics of the reflection coefficient via fast Fourier transform (FFT), and analyze the film thickness by combining the resonance model or spring equivalent model [116, 124, 144]. However, the ultrasonic method is limited by its acoustic wave characteristics and requires innovative algorithms for effective compensation of reference signals.

4 Performance influencing factors and optimization design of thrust bearings

Hydrodynamic thrust bearings have been widely used in engineering due to their characteristics of high stability, reliability, ease of manufacturing, and diverse types. However, they exhibit problems during design and operation, such as excessive deformation of bearing pads affecting hydrodynamic pressure generation, uneven load distribution, and insufficient load-carrying capacity. To reduce losses caused by surface friction and prolong their service life, numerous studies have focused on optimizing the lining material of bearing pads to enhance their wear resistance and friction reduction properties, while introducing surface texturing technology to the pad surface to improve the lubrication state. Therefore, this section analyzes the influence of bearing pad lining materials and surface textures on the lubrication performance of hydrodynamic thrust bearings.

4.1 The influence of bearing pad lining materials on thrust bearing performance

Bearing pad surfaces of thrust bearings in large-scale equipment are often coated with Babbitt metal (a soft alloy) as the lining layer. Babbitt metal exhibits excellent anti-friction, anti-seizure, embedability, and running-in properties [145-147]. Brown et al. [148] investigated the hydrodynamic lubrication limit of large spring-supported thrust bearings in hydro-generators through experiments, and pointed out that such bearings with Babbitt metal linings can still maintain low-friction hydrodynamic lubrication at speeds as low as 10 rpm. Industrial practice shows that Babbitt metal bearings can still operate safely even when the sliding speed reaches 3 m/s, and the allowable minimum rotational speed of larger-sized bearings may be lower [149]. In large-scale thrust bearings, Babbitt metal pads are designed with a single-layer or double-layer structure, whose thickness is approximately 4–6 mm. The oil inlet edge of the bearing pads generally has a relatively large slope to facilitate the entry of lubricating oil into the pad surface during bearing start-up. Meanwhile, high-pressure oil jacking devices need to be equipped to facilitate the start-up and shutdown of the bearing system. However, Babbitt metal has drawbacks such as low melting point and poor fatigue strength. Under high-temperature conditions, it will creep due to reduced strength, leading to significant thermal convex deformation of the pads. Guo et al. [145] found that when the temperature is below 130°C, the content of α-Sn phase in the Babbitt metal surface remains stable, at which point the wear rate is relatively low, and the wear form is mainly mild wear characterized by the coexistence of plastic deformation and abrasive wear. While when the temperature exceeds 130°C, the content of α-Sn phase decreases significantly, and the hard Cu_6Sn_5 phase increases remarkably, leading to a substantial rise in the wear rate and the transformation of the wear mechanism into severe melting wear.

With the increasing requirements for the performance and efficiency of thrust bearings in industrial production, the aforementioned issues have limited the application of Babbitt metal bearings. Thus, scholars have paid increasing attention to and conducted more research on polymer liners, among which polytetrafluoroethylene (PTFE) and PEEK are two typical materials. Studies show that compared with Babbitt metal, polymers such as PTFE and PEEK have higher specific pressure and lower friction coefficient [150, 151]. Table 4 summarizes the dominant failure modes and prediction methods for Babbitt-lined and polymer-lined thrust bearings.

Table 4 The dominant failure modes and prediction methods for Babbitt-lined and polymer-lined thrust bearings

Type	Dominant failure mode	Model prediction method	Experimental prediction method**	Practical monitoring method
Babbitt-lined thrust bearing	1. Fatigue spalling and cracking under cyclic loading. 2. Bearing burn-out due to localized high temperature. 3. Scoring/galling of metal interfaces under high temperature and pressure. 4. Direct metal-to-metal wear following oil film failure. 5. Surface corrosion and cavitation erosion caused by oil degradation and water/gas entrainment.	1. TEHD model based on Reynolds equation for thrust bearing lubrication prediction. 2. CFD simulation of thrust bearing lubrication characteristics under complex operating conditions. 3. Big data-driven AI prediction method	1. Accelerated life test. 2. Oil contamination test: Measure friction, wear, corrosion, and other phenomena under conditions of different oil types, water/gas content, and abrasive particles. 3. Material high-temperature performance test. 4. Creep test. 5. Extreme operating condition test.	1. The monitoring of various parameters* and the handling of related tasks through online/offline oil monitoring technology. 2. Monitoring of unit vibration and operating conditions through relevant technologies.
PTFE-lined thrust bearings	1. Plastic deformation under prolonged high specific pressure. 2. Local bulging or warping due to uneven temperature rise. 3. Accumulation of frictional heat and material degradation. 4. Wear and delamination.			
PEEK-lined thrust bearings	1. Abrasive wear induced by hard particles in the oil. 2. Material softening due to accumulated frictional heat. 3. Severe wear under harsh operating conditions.			

*: In addition to the monitoring parameters described in Section 3.1.2, parameters such as viscosity, moisture, contamination level, and ferromagnetic particle content are included.

**: Testing is required based on the applicable operating conditions for thrust bearings with three different liner types.

4.1.1 PTFE liner

PTFE is generally classified as a material suitable for dry sliding conditions. Its friction coefficient against steel can be as low as 0.05 (depending on the load and surface finish), with an extremely low wear rate. PTFE-faced thrust bearings successfully replaced Babbitt metal bearings in the field of hydropower generators in the Soviet Union and China in the 1970s, and have since been widely adopted. Long-term operating results show that the liner surfaces remain smooth and free from severe wear, delamination, or warping (**Fig. 12**), which fully demonstrates the excellent service performance of PTFE liners [152].

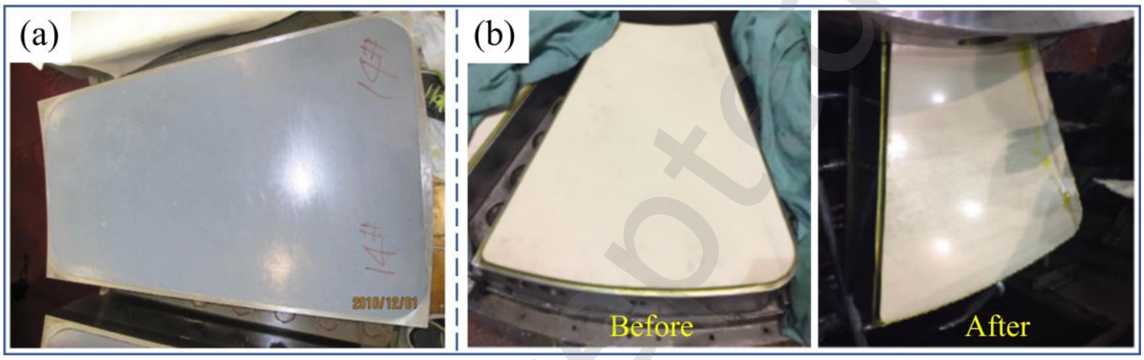

Fig. 12 (a) The condition of the surface of the elastic metal plastic pads after 15 years of operation; (b) Comparison of the elastic metal plastic pads before and after maintenance [152].

Early research has demonstrated that PTFE liners exhibit a significantly lower thermal gradient across the thickness direction and superior thermal insulation compared to Babbitt metal liners. Owing to the lower thermal conductivity and more uniform temperature distribution of PTFE, such liners result in reduced pad thermal crowning, lower maximum oil film pressure, and reliable performance under high specific loads [153-156]. In terms of hydrodynamic lubrication, studies by Ettles et al. [153] and Fang et al. [157] indicated that there were no significant differences in oil film temperature and power loss between PTFE liners and Babbitt metal liners, with similar oil film thickness. However, PTFE liners exhibit superior pressure distribution characteristics: the oil film pressure is significantly reduced and more uniformly distributed, while the pad temperature and overall thermal deformation are substantially decreased. It is worth noting that in the simulation conducted by Fang et al. [157], the thickness of the PTFE layer was much larger than that of the Babbitt alloy layer (approximately 2.5 times thicker), which may further enhance its lubrication performance. Although there is no significant difference in oil film thickness between different liner materials under hydrodynamic lubrication conditions, polymer liners exhibit superior lubrication performance with lower static friction under boundary lubrication conditions [158].

The geometric shape and thickness parameters of the PTFE material layer are key factors determining the performance characteristics of PTFE-faced thrust pad bearings. Glavatskih et al. [159] indicated that the thickness of the PTFE layer significantly influences the oil film temperature. When the thickness increased from 0.5 mm to 2.0 mm, the maximum oil film temperature rose from 89°C to 94°C. The predictions of the TEHD model exhibited excellent agreement with the experimental data, which validated the reliability of the model. Further systematic studies comprehensively investigated the combined effects of liner geometric characteristics and PTFE layer thickness on thrust bearing performance, as shown in **Fig. 13**. Specifically, increasing the length and height of the taper lands was found to reduce both the minimum oil film thickness and the maximum temperature, while simultaneously leading to an increase in the maximum oil film pressure. In contrast, an increase in PTFE layer thickness caused the maximum temperature to rise, accompanied by a decrease in both the minimum oil film thickness and the maximum oil film pressure. Furthermore, power loss was only slightly affected by variations in these two sets of parameters [160]. Wang et al. [156] investigated the thickness matching relationship between the PTFE layer and the steel substrate in large thrust bearings based on a 3D TEHD model. The results indicated that when the PTFE layer thickness exceeded 0.5 mm, a contracted zone appeared in the radial mid-region of the oil film pressure distribution. This zone expanded with increasing PTFE thickness, accompanied by a pronounced reduction in pressure. Although the minimum pressure was observed for a PTFE layer thickness of 6 mm, an excessively thick PTFE layer led to an overly thin oil film in the central region, which is unfavorable for maintaining full-film lubrication. Consequently, the study recommended an optimal design parameter in which the thickness ratio of the PTFE layer to the steel substrate is 0.0375.

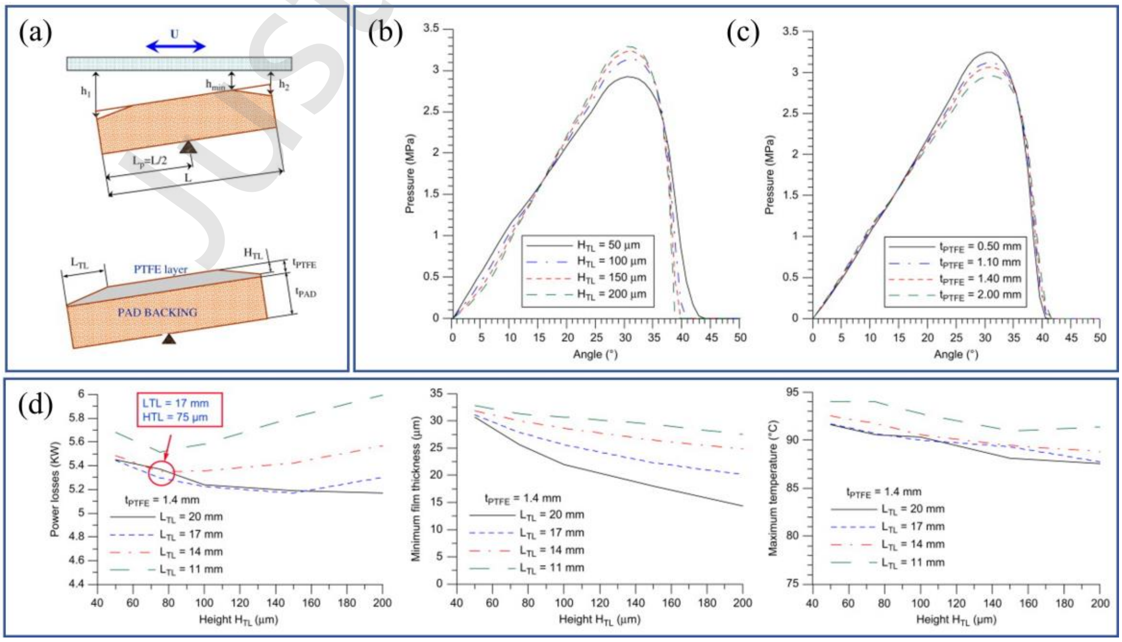

Fig. 13 Effect of geometric characteristics and thickness of PTFE liner on thrust bearing performance [160]. (a)

Thrust pad support structure and PTFE liner geometric characteristics; (b) Pressure profiles for different heights of the taper land at L_{TL}=17 mm and t_{PTFE}=1.4 mm; (c) Pressure profiles for different thicknesses of the PTFE liner at L_{TL}=17 mm and H_{TL}=75 μm; (d) Effect of PTFE liners with different taper lengths on bearing characteristics.

4.1.2 PEEK liner

PEEK is a special engineering plastic that possesses excellent properties such as high temperature resistance, self-lubrication, wear resistance, and high mechanical strength [161]. In practical applications, PEEK has limitations including insufficient surface adhesion, inadequate wear resistance for engineering requirements, and difficulty in processing and forming; therefore, it is often modified to produce PEEK composites with more comprehensive performance. Mitsubishi Heavy Industries developed a high specific pressure thrust bearing using PEEK resin gaskets. Incorporating direct lubrication technology, this bearing can reduce the diameter of the rotor thrust disc to minimize steam leakage and improve steam turbine efficiency. Verified through 29-inch full-scale bearing tests (maximum specific pressure of 12 MPa, temperature up to 161°C) and 6-year long-term operation in internal power plants (20,462 hours, 631 start-stops), its reliability is superior to that of traditional Babbitt metal bearings, and its maximum allowable specific pressure is 1.5–2 times that of Babbitt metal [162]. Zhou et al. [163] investigated the performance of TPTBs with PEEK and Babbitt metal liners under high-speed oil lubrication. At 11,000 rpm, the load-carrying capacity of PEEK liner bearings (14.5 MPa) was 51% higher than that of Babbitt metal-lined ones (9.6 MPa), while their temperature and power loss were comparable to those of Babbitt metal bearings. Bouyer et al. [164] experimentally studied the friction torque of thrust bearings during start-up, which included the effects of load, bearing size, and bearing liner material. They found that the start-up torque of PEEK bearings was much lower than that of Babbitt metal bearings. Wasilczuk et al. [118, 165] experimentally investigated the performance of TPTBs with four different material combinations (**Fig. 14(a)**) under specific operating conditions. The tests included loaded shutdown tests and reproducing the stribeck curve by reducing the rotational speed to an extremely low value. The results showed that DLC-steel bearings exhibited a lower friction coefficient, could transition to mixed lubrication under higher loads, and had more stable performance during start-stop conditions; PEEK-steel bearings ranked second; the traditional bronze-steel and Babbitt metal-steel combinations had higher friction coefficients and earlier transitions, as shown in **Figs. 14(b)** and **(c)**.

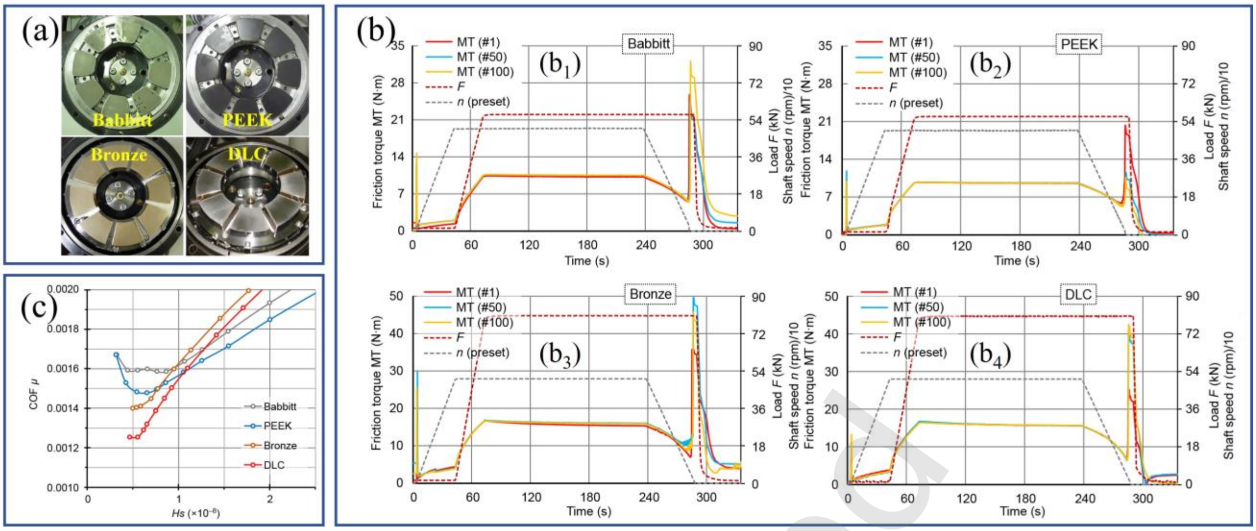

Fig. 14 (a) Photographs of the test bearings; (b) Friction torque of different material bearings in start-stop cycles; (c) The relationship between COF and *Hs* [118].

Koosha et al. [48] investigated the influence of different materials on the static load performance of TPTBs under flow regimes ranging from laminar to turbulent. As shown in **Fig. 15**, under laminar conditions, Babbitt thrust bearing exhibited the largest oil film thickness and the lowest temperature rise. In contrast, under turbulent conditions, full-hard polymer thrust bearing demonstrated the largest film thickness and the lowest drag power loss. Ricci et al. [166] compared the performance of Babbitt metal bearings and polymer-lined bearings (PTFE and PEEK) via multiphysics modeling, and obtained interlayer and bearing deformations, oil film thickness, temperature, and pressure distributions under different operating conditions. Similar to PEEK, PTFE also exhibits liner deflection at the center of the pad, leading to a significant reduction in minimum oil film thickness [153, 159]. Studies on the variation of apparent Young's modulus of two composite polymer liners with temperature showed that, within the range of 25°C–120°C, the apparent Young's modulus of PTFE-based composite liners decreased from 361 MPa to 84 MPa (a 4.3-fold reduction) with significant creep; in contrast, that of PEEK-based composite liners decreased from 2715 MPa to 2340 MPa (only a 1.16-fold reduction) with almost no creep [167]. Obviously, PEEK is more suitable for heavy-load conditions. In addition, compared with PTFE-liner thrust pads, PEEK-liner thrust pads have higher stiffness and lower damping, making them more suitable for working conditions requiring high stiffness and low damping. And PEEK performs slightly better in suppressing the impact of thermal deformation on bearing performance [155].

To summarize, the selection of bearing liner materials directly determines the performance boundaries and application scenarios of hydrodynamic thrust bearings. Babbitt metal remains irreplaceable in low-speed, medium-load operations due to its excellent anti-friction and running-in properties, but fails to meet high-temperature/heavy-load demands. Polymer liner materials exhibit greater adaptability and development potential, and are widely used to replace Babbitt metal in hydraulic turbines. Currently, bearing materials tend toward composites: elastic metal-plastic liners combine rigid support and flexible adaptability, while new materials like carbon fiber-reinforced PEEK further push performance limits, providing reliable material support and technical paths for thrust bearings under complex conditions.

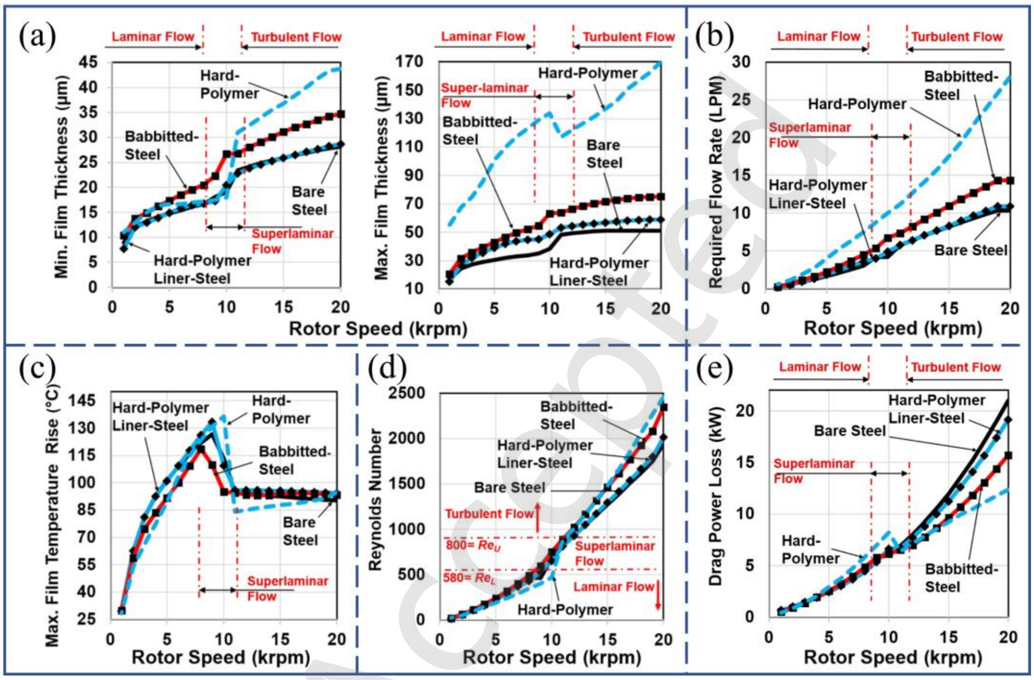

Fig. 15 The relationship between the performance of four types of thrust pads and the variation of rotor speed [48]. (a) Minimum film thickness and maximum film thickness; (b) Drag power loss; (c) Maximum film temperature rise; (d) Circumferential Reynolds number; (e) Supply flowrate.

4.2 Surface texture

To reduce friction and wear on thrust bearing surfaces, enhance their load-carrying performance, and extend their service life, numerous studies have introduced surface texturing technology into thrust bearings. Surface texturing refers to micro-nano patterns with specific shapes, sizes, and arrangements that are fabricated on workpiece surfaces via specific processing methods. Benefiting from the exploration of non-smooth surfaces of natural organisms, an increasing number of bionic micro-texture patterns have been developed and applied to friction pair surfaces [168-171], and the research system of surface texturing has also been continuously improved. Surface texturing involves various processing technologies, among which laser surface texturing (LST) is widely adopted due to its advantages of high efficiency, environmental friendliness, and strong operability [88, 172]. The main advantage of surface texturing in improving thrust bearing performance lies in its "additional hydrodynamic lubrication effect," whose basic principle for generation is the "cavitation effect" [173, 174]. Additionally, texturing also has lubricant storage and wear debris collection functions [175-177], which can increase the film thickness between friction pairs and reduce wear. The anti-friction and anti-wear mechanism of the surface texture is illustrated in Fig. 16.

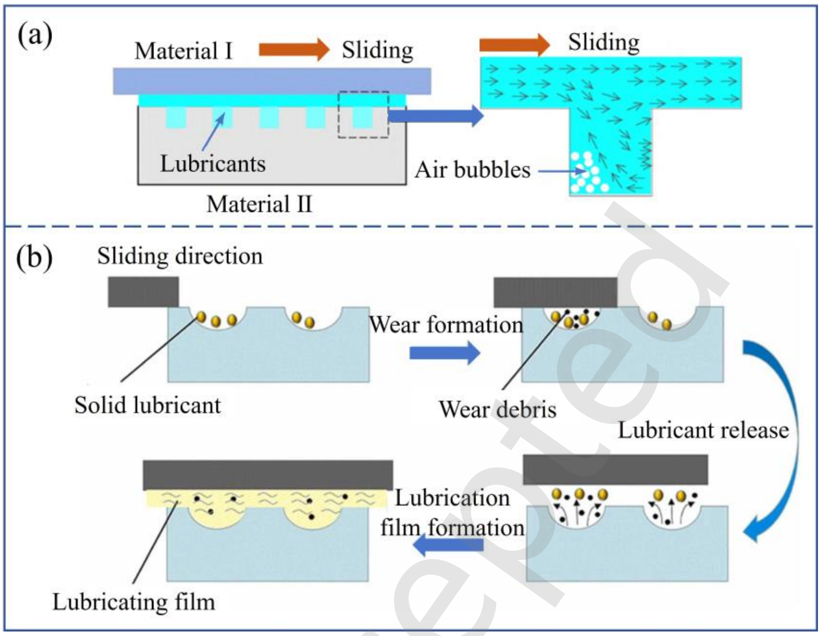

Fig.16 The anti-friction and anti-wear mechanism of the surface texture. (a) Hydrodynamic lubrication effect[174]; (b) Lubricant storage and wear debris collection functions[177]

Most studies on textured thrust bearings are based on different forms of the Reynolds equation or N-S equations. The validity of the Reynolds equation is closely related to the Reynolds number (*Re*) and texture aspect ratio [178]. It is applicable to cases with shallow textures and small *Re*, while the N-S equations are required for deep textures. Additionally, inertial effects reduce the load-carrying capacity in locally arranged textured sliders, and texture unit models cannot accurately evaluate these effects. With the development of more efficient algorithms and solution techniques, more influencing factors (including turbulence effects, cavitation effects, viscosity-temperature variation, and inertial effects) have been gradually incorporated into the theoretical research on surface textures of thrust bearings, which greatly improves model accuracy [67, 179-181].

Under complex operating conditions, mechanical and thermal deformations of textured thrust bearings significantly affect their performance. Since existing calculation methods may overestimate the actual performance of textures, it is necessary to investigate the effects of thermal and mechanical deformations on textured thrust bearings optimized via the T(E)HD method [182]. **Fig. 17** shows the comparison of results for the optimal texture parameters (obtained via optimization) between THD and TEHD simulations [183]. In TEHD simulations, the oil temperature is lower than that in THD; additionally, the bearing load-carrying capacity is reduced by 13% and the friction coefficient is increased by 10% compared with THD results. This indicates that thermal and mechanical deformations exert a significant influence on the performance of textured thrust bearings. In practical applications, it is recommended to first optimize parameters via THD, then use TEHD simulations to fine-tune geometric details and quantify performance indicators.

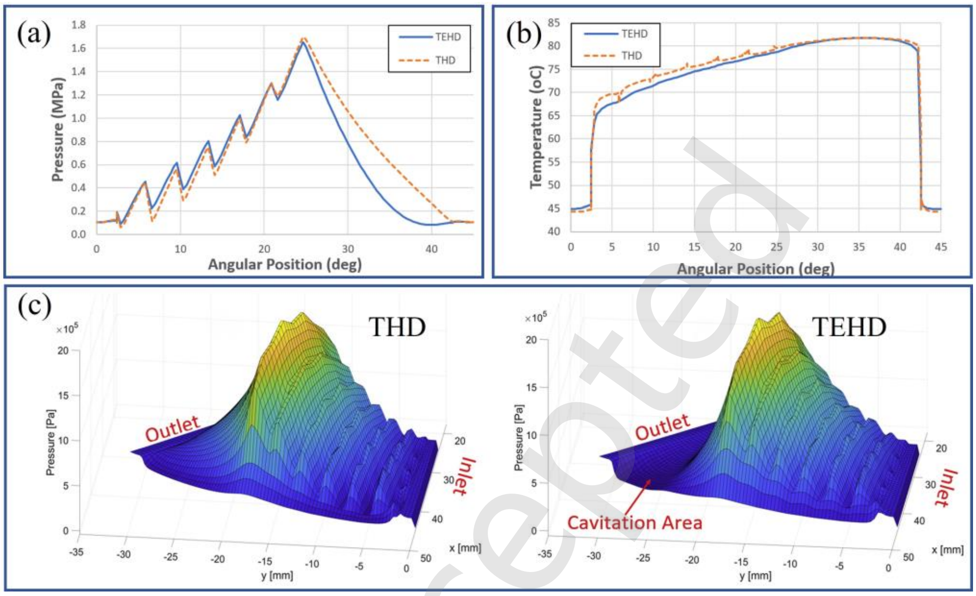

Fig. 17 (a) Pressure profiles of the TEHD and THD models at a radius of 34 mm; (b) Pressure profiles of the TEHD and THD models at a radius of 34 mm; (c) 3-D pressure field at fluid/pad interface [183].

4.2.1 Study on the shape and key parameters of surface texture

Texture shape, design parameters, and position arrangement/distribution are the main factors influencing the tribological performance of surface textures. **Figs. 18(a)–(c)** show the morphological characteristics of some common conventional surface textures. Yun et al. [184] fabricated bionic dimple textures on polycrystalline diamond compact (PDC) via laser machining, optimized their spacing, diameter, and depth through orthogonal experiments, and concluded that the optimal parameters were 1,000 μm spacing, 45 μm diameter, and 30 μm depth. The friction coefficient and temperature of textured PDC were reduced by a maximum of 29.11% and 16.88%, respectively, as shown in **Figs. 19(a) and (b)**. Lu et al. [92] proposed a new dimple arrangement method based on phyllotaxis theory. They experimentally investigated the friction coefficients under different dimple arrangements and phyllotaxis coefficients, as shown in **Figs. 19(c) and (d)**. The results indicated that when the phyllotaxis coefficient was 2.4 and the dimple diameter was 2 mm, the friction coefficient was reduced by a maximum of 27%. Additionally, compared with radial scattering patterns and staggered patterns (**Fig. 18(b)**), thrust bearings with phyllotactic-patterned dimples exhibited better lubrication performance. This is attributed to their excellent position compensation, no lubrication blind areas, and consequent uniform oil film formation.

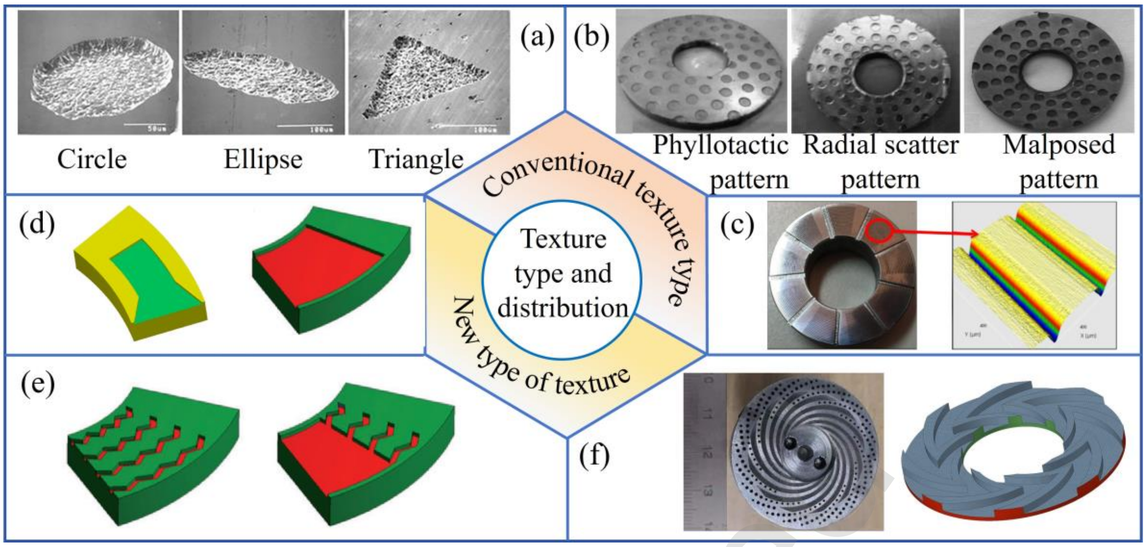

Fig. 18 Types and distribution of different textures. (a) Surface texture of different shapes[185]; (b) Dimpled thrust bearings[92]; (c) The morphology of the circular grooves[88]; (d) New pocketed pad[186] and pocketed pad[187]; (e) Fish scale textured pad and pocketed-fish textured pad[187]; (f) Textured spiral groove thrust bearing[188] and herringbone groove thrust bearing[189]

Texture distribution range also influences the lubrication performance of thrust bearings, with partial and full textures exhibiting significant differences in effectiveness. Brizmer et al. [190] conducted a theoretical study on textured thrust bearings and concluded that compared with fully textured surfaces, partially textured surfaces can further enhance load-carrying capacity. Their conclusion was verified by Etsion et al. [191], who found that the friction force of partially textured bearings was significantly reduced. For the distribution range of partial textures, the optimal range varies with texture types, parameters, and optimization objectives. Spherical textures achieve maximum load-carrying capacity with 50% circumferential coverage and 90%–100% radial coverage [192]. Generally, optimal bearing performance is achieved with rectangular textures at a circumferential coverage of 39%–74% and radial coverage of 56%–91% [182]. CFD simulations indicate that both rectangular and elliptical dimples achieve optimal radial texture distribution at 80% of the bearing pad radial length, while the circumferential length of elliptical dimples is 30% larger than that of rectangular ones. The two textures exhibit nearly identical load-carrying capacity, but elliptical dimples have a slightly lower temperature [193]. Chen et al. [88] conducted theoretical and experimental studies on partially textured thrust bearings with circular grooves. The results showed that partially textured thrust bearings outperform fully textured ones, especially under high rotational speeds and low loads. The dimensionless circumferential range depends on the depth of circular grooves, and load-carrying capacity decreases with increasing spacing between adjacent grooves. Furthermore, for groove-type textures, the lubrication performance of circumferential grooves is superior to that of radial grooves. Among these, the optimal circumferential coverage ratio is 50%, at which the oil film load-carrying capacity and anti-friction effect reach the best level; the radial coverage ratio is recommended to be controlled within the range of 60%-80%, which enables a balance between oil storage capacity and oil film stability[194].

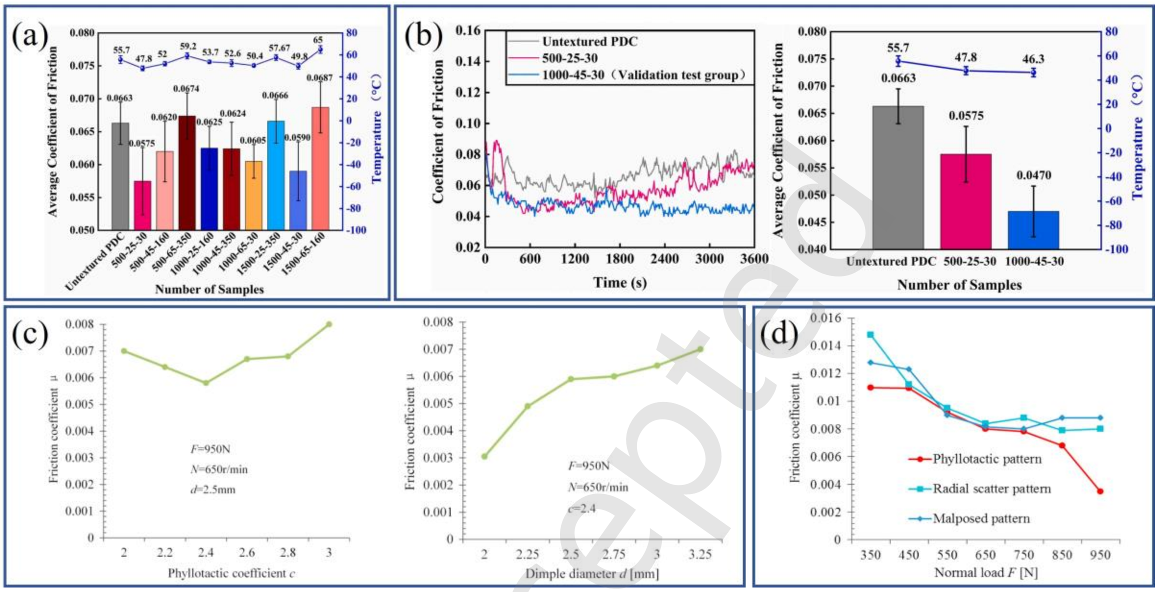

Fig. 19 (a) Comparison of average COF and temperature of textured PDC [184]; (b) Comparison of COF and temperature between the optimized test group and other test groups [184]; (c) Effects of different phyllotactic coefficients and dimple diameters on the COF of different dimpled thrust bearing specimens [92]; (d) Effects of three dimple distribution patterns on the COF under different loads [92].

In comparative studies on texture shapes, performance differences between textures of different morphologies become more apparent. Yu et al. [185] found that under the same parameters, elliptical dimples perpendicular to the sliding direction exhibit better load-carrying capacity than circular textures. Kumar et al. [195] further conducted finite element simulations on thrust bearings with a combination of elliptical dimple textures and rough surfaces; after parameter optimization, the bearing load-carrying capacity and oil film stiffness coefficient increased by 91.3% and 98.8%, respectively. Although numerous studies have explored the influence of surface texturing on the tribological performance of thrust bearings, most focus on dimpled textures, while application research on protruded textures remains limited. Panigrahi et al. [196] experimentally investigated the effects of size and height of four positive textures (circular, elliptical, square, and triangular) on the tribological performance of thrust bearings. They found that textures with small size and large height exhibited lower friction torque and larger bearing clearance, outperforming non-textured surfaces. However, this study did not compare positive and negative textures, thus failing to determine their superiority under specific operating conditions. In addition to the optimization of conventional textures, innovative designs of new texture shapes also provide new insights for thrust bearing performance enhancement. Atwal et al. [186, 187, 197, 198] have conducted a series of studies on the performance optimization of new textured thrust bearings (**Figs. 18(d) and (e)**). Integrating numerical simulation methods (accounting for cavitation, thermal effects, turbulence, etc.), they systematically investigated the influence of structural parameters on key bearing performance under different lubrication media, bearing types, and operating conditions. The results show that compared with conventional smooth pads or rectangular cavity pads, the optimized surface textures significantly improve thrust bearing performance: increasing the minimum oil film thickness by 10%–270% and reducing the friction coefficient or power loss by 5%–24%. Meanwhile, the studies indicate that structural parameters need to be optimized for specific scenarios; excessive increases in parameters such as texture depth will lead to performance degradation.

4.2.2 Numerical optimization design of textures

As mentioned above, conventional studies typically rely on limited parameters to define texture types and their distribution, adopting the trial-and-error method or statistical experimental design (DOE) to identify optimal parameter ranges. Although the trial-and-error method is easy to operate, it is not only time-consuming and labor-intensive but also has a limited effect on improving lubrication performance. In recent years, researchers have proposed adopting numerical optimization methods [199, 200] to improve the tribological performance of friction pairs by optimizing surface texture parameters, providing a new approach for research in this field. Compared with conventional trial-and-error approaches, optimization algorithms can rapidly identify optimal texture shapes and distributions under varying operating conditions based on well-defined performance objectives, thereby significantly improving design efficiency and reducing resource expenditure. Moreover, the texture types and distributions obtained through optimization algorithms exhibit notable differences from those derived via traditional design methods. The resulting texture parameters demonstrate stronger adaptability to operational conditions, whereas traditional design methods struggle to achieve this specific type of texture structure and distribution. **Table 5** summarizes the numerical optimization and analysis methods for textured thrust bearings in different literatures.

Zhang et al. [201, 202] characterized the distribution of circular micro-textures using a rectangular grid matrix and optimized texture parameters via the genetic algorithm (GA). They concluded that the pyramid-shaped distribution at the inlet is optimal, and sliders with small width and small convergence ratio show significant performance improvement. Experimental verification shows that the optimized texture distribution exhibits a lower COF and higher load-carrying capacity. The comparison between simulation and experimental results is as shown in **Fig. 20**.

Although the GA has strong global search capability, its local search capability is weak. Wang et al. [203] constructed a numerical model based on the JFO cavitation condition and the GA-SQP hybrid algorithm. This model strengthened local search capability via the SQP algorithm, and finally identified that the optimal shape of groove textures under different rotational speeds is V-shaped. Under specific operating conditions, it achieves a stable ultra-low COF < 0.01. However, for simplicity, the area ratio of groove textures was fixed at 25.0%. Thus, the optimized shape is only a local optimal solution rather than a global one. Building on this foundation, Li et al. [204] further optimized the geometry and area ratio of surface textures using this optimization model, concluding that under different rotational speeds and area ratios, the optimal groove texture is a V-shape with a flat front, and the optimal area ratio is 40.4%. Beyond the design parameters of textures themselves, texture position distribution also significantly affects the load-carrying capacity (LCC) of the lubricating film. In a recent study, Li et al. [94] comparatively analyzed the optimal distribution and performance of flat-headed chevrons and circular dimples under different quantities and rotational speeds. The results show that the optimal distributions of flat-headed chevrons and circular dimples exhibit asymmetric wedge shapes and chevron shapes, respectively (as shown in **Fig. 21**). The optimal distributions improve LCC and reduce COF via the collective effect.

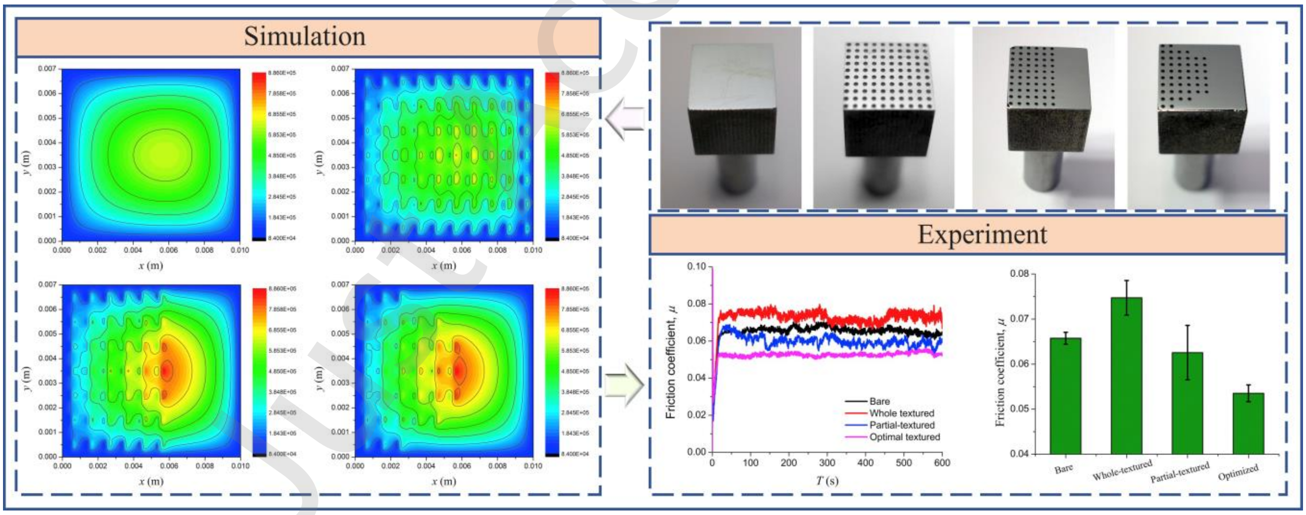

Fig. 20 Photographs, pressure distributions, and the COF of thrust bearing sliders with smooth surface, whole-textured surface, partial textured surface, and optimal textured surface [201].

None of the aforementioned studies have considered thermal effects. Yu et al. [205-208] established thrust bearing models with different texture types based on the modified Reynolds equation. They systematically studied the influences of texture parameters (width, depth, quantity, spacing) on oil film temperature and pressure, and adopted multiple improved optimization algorithms based on BP neural networks (**Table 5**) to conduct multi-objective optimization of oil film temperature and load-carrying capacity, accounting for the effects of variable viscosity, turbulence, and cavitation on the fluid physical field. The results show that textured thrust bearings outperform non-textured ones: circular textures exhibit the optimal load-carrying capacity (increased by approximately 28.8%) and frictional performance (COF reduced by approximately 18.9%), while triangular textures show the most significant temperature improvement (reduced by approximately 1.93%). Notably, although the aforementioned studies have incorporated thermal effects and achieved performance optimization under steady-state conditions, the dynamic characteristics and friction states of thrust bearings in specific operating conditions change significantly during operation and are mutually coupled—and this transient effect has not been reflected in previous optimizations. Among various transient conditions, the start-up and shutdown processes are particularly critical and warrant primary focus, as they are inevitable operational phases where bearings are prone to severe boundary lubrication and wear. Therefore, conducting texture optimization analysis that specifically addresses these critical transient phases is essential to enhance operational safety and reliability [209].

It should be noted that when applying optimization algorithms to texture design, the variable ranges must be properly constrained, and practical manufacturability must be taken into account to prevent idealized designs from exceeding feasible production capabilities, thereby ensuring that optimized results balance performance enhancement with engineering viability.

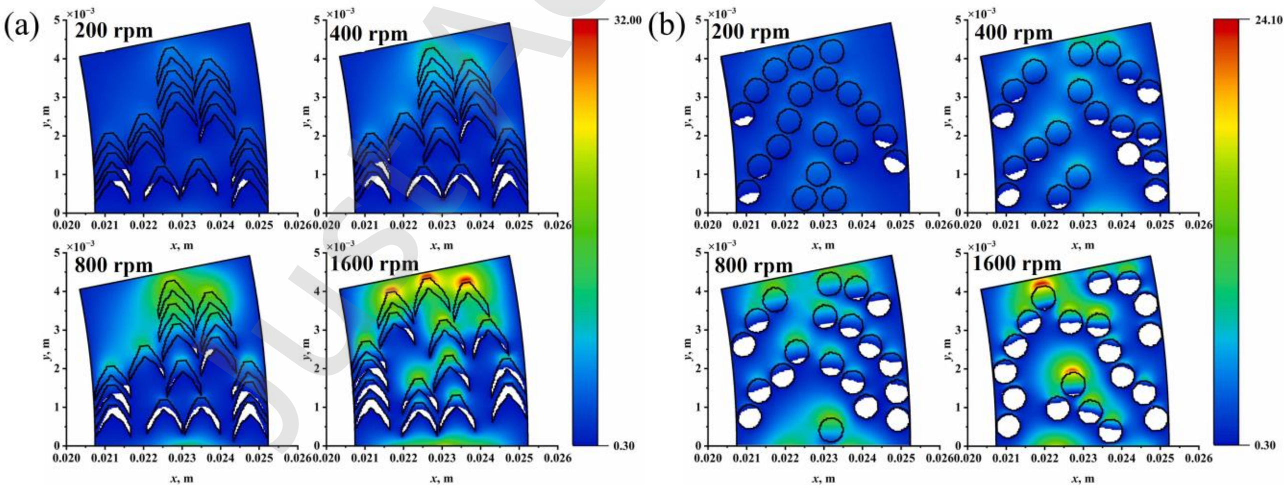

Fig. 21 The optimal texture distribution and corresponding pressure distribution at different rotational speeds [94]. (a) Flat-headed chevron; (b) Circular texture.

Table 5 Numerical optimization design and analysis methods for textured thrust bearings

Ref.	Methods	Operating parameters	Texture type and parameters	Optimize parameters	Core optimization indicators	Optimization algorithm	Others
[201]	» HD analysis based on the Reynolds equation	8 N and 0.2 m/s	» circular texture » Φ=0.4 mm, D=0.01 mm, S=1 mm	The optimal distribution of the texture	COF	GA	All algorithms are single-objective optimization algorithms. GA has strong global search; SAA avoids local optima; PSO features fast convergence; GA-SQP balances global search and local optimization accuracy.
[203]	» HD analysis based on the Reynolds equation	200-1,600 rpm and 300N	» groove texture » The area ratio is 25.0% and λ=1	The optimal profile of the texture	LCC	GA-SQP	
[183]	» THD and TEHD analysis based on N-S equation	6,000 rpm	» rectangular texture » The texture density is 80%.	The optimal L, W, D and texture proportion of the texture	LCC and the friction torque	GA	
[209]	» EHD analysis based on the Reynolds equation	30 Hz and 90 Hz	» irregular texture	The optimal shape and D of the texture	Wear load	GA; PSO; SAA	
[206]	» THD analysis based on the Reynolds equation » consider the turbulence effect	180 rpm	» circular texture » Φ=0.1、0.2、0.3 mm; D=0.1、0.3、0.5 mm; S=2、3、4 mm; Q=30、32、34	The optimal Φ, D, S and Q of the texture	Oil film temperature and LCC	BP-IMOALA	All algorithms are hybrid intelligent optimization algorithms integrating BP neural networks and improved multi-objective swarm intelligence algorithms.
[207]			» triangular texture » W=0.14、0.27、0.4 mm; D=0.1、0.3、0.5 mm; S=1、2、4 mm; Q=30、32、34	The optimal W, D, S and Q of the texture		BP-IMODA	
[208]			» square texture » W=0.09、0.18、0.27 mm; D=0.1、0.3、0.5 mm; S=1、2、3 mm; Q=30、32、34	The optimal W, D, S and Q of the texture		BP-IMOSSA	
[210]	» EHD analysis based on the Reynolds equation » dynamical model	200–1,600 rpm and 300 N	» spherical texture	The optimal Φ and D of the texture	LCC; torque loss; leakage rate	NSGA - II; MO-ASMO	All algorithms are multi-objective optimization algorithms. MO-ASMO is endowed with advantages in optimization accuracy and convergence efficiency.
[211]	» HD analysis based on the Reynolds equation	8,000 rpm	» rectangular texture	The optimal L, W, D, S and distribution of the texture	LCC and friction force	NSGA-II-RSM	

Notes: Selection of optimization algorithms should be adapted to the complexity and structural characteristics of the target problem. For single-objective performance optimization, single-objective optimization algorithms are recommended if the computational cost is low and the design variables are moderate-dimensional. When multiple performance indicators require simultaneous optimization, multi-objective optimization algorithms become necessary. In cases involving numerous design variables, strong nonlinearity, and high computational or experimental costs, optimization algorithms integrated with surrogate models are recommended. Among these, hybrid intelligent approaches that integrate neural networks with intelligent algorithms can approximate complex performance mappings, predict objective values rapidly, and balance computational accuracy and efficiency.

5 Conclusions

As a key supporting component in high-end equipment, hydrodynamic thrust bearings have lubrication performance and service reliability that directly affect the operational efficiency and safety of the entire machine. This paper systematically reviews the development of lubrication theory, multi-physics coupling modeling, performance testing technology, and optimization design methods for hydrodynamic thrust bearings. The main conclusions are as follows:

(1) The lubrication theory of hydrodynamic thrust bearings has gradually developed from HD models to TEHD models that integrate thermal effects and elastic deformation. The development of CFD technology has broken through the limitations of the traditional Reynolds equation, significantly improving computational accuracy and the ability to handle complex operating conditions. By further considering complex factors such as turbulence and cavitation based on the aforementioned models, the engineering applicability of the models has been significantly enhanced, providing a reliable theoretical basis for performance prediction and structural optimization of thrust bearings under complex operating conditions.

(2) Experimental evaluation and verification are a necessary step to reveal the lubrication characteristics of hydrodynamic thrust bearings. Basic tribological experimental setups are used to study the micro-scale friction and wear behavior of materials and structures, clarifying the relevant friction and wear mechanisms. Full-scale bearing test rigs enable the dynamic monitoring of parameters such as oil film pressure, temperature, and thickness. The application of advanced detection technologies has improved testing accuracy, providing precise measured data for the calibration of numerical models.

(3) The liner materials of thrust bearing pads have been gradually expanded from traditional Babbitt metal to polymer composites such as PTFE and PEEK, significantly enhancing the load-carrying capacity and wear resistance of bearings. Surface textures demonstrate great potential for improving the tribological performance of hydrodynamic

thrust bearings under different application scenarios and operating conditions. The introduction of numerical optimization algorithms has enabled efficient optimization of texture parameters, which can quickly converge to the global optimal solution, thereby achieving the best tribological performance.

6 Future prospects

Although significant progress has been made in the research on hydrodynamic thrust bearings, in response to the development demands of high-end equipment for higher speed, heavier load, and longer service life, there remains a need to deepen exploration in the following areas:

(1) Although THD and TEHD analyses methods have laid a theoretical foundation for studying the lubrication performance of hydrodynamic thrust bearings, their actual operation is influenced by the combined effects of multi-physics coupling and transient conditions. Therefore, it is imperative to develop integrated thermo-elastohydrodynamic models that incorporate multiple factors, with particular emphasis on deepening the study of lubrication characteristics during transient processes such as start-up and shutdown, and extending the model's applicability across various working conditions and lubrication states. Furthermore, it is essential to advance coupled models of fluid lubrication and structural dynamics to elucidate the interaction mechanisms between the oil film and the dynamic behavior of the bearing-rotor system during operation, thereby providing a theoretical basis for improving operational stability and reliability. Concurrently, algorithmic optimizations are required to address the trade-off between accuracy and efficiency in multi-physics, multi-scale coupling analyses.

(2) The integration of data-driven methods with physical constraints has demonstrated significant potential in modeling and predicting sliding bearing systems involving multiphysical parameters and complex structures [212-215]. However, its application remains in the early exploratory stage. Future efforts should further incorporate the core structural features of thrust bearings, along with optimization strategies such as periodic boundary condition embedding and adaptive collocation sampling, to achieve efficient and generalizable intelligent lubrication prediction models.

(3) The integration of computational methods and experimental validation has become a core approach for revealing the lubrication characteristics of hydrodynamic thrust bearings. However, existing experimental setups exhibit limited capability in monitoring parameters under complex operating conditions. It is therefore necessary to develop thrust bearing test platforms integrated with multi-sensor arrays to achieve distributed dynamic measurement of bearing performance. Furthermore, with the advancement of Internet of Things and sensing technologies, the construction of a digital twin system for thrust bearings has become a key direction for achieving intelligent operation

and maintenance along with predictive maintenance. By integrating real-time monitoring data with multiphysics coupling models, the digital twin enables dynamic mapping of bearing status and performance prediction. Future research should focus on establishing a bidirectional coupling mechanism between high-fidelity simulation models and real-time data, utilizing machine learning methods to calibrate model parameters, and developing a fault warning and remaining life assessment system based on the digital twin.

(4) Current research on polymer composites is mostly focused on fundamental exploration and lacks correlation verification with practical operating conditions. Future efforts should strengthen operational testing in model test rigs to evaluate their practical service performance. Additionally, linking macroscopic experimental data to microscopic mechanisms, along with integrating multi-scale theoretical models to reveal the intrinsic tribological laws of materials, constitutes a key research direction. Meanwhile, modification methods for polymer composites must be further advanced to overcome existing performance limits. In light of the increasing emphasis on sustainability, the environmental performance assessment of materials and the development of green lubrication technologies also represent important future avenues in thrust bearing research.

(5) Optimal texture parameters under different operating conditions differ significantly. It is necessary to integrate numerical optimization methods for efficient optimization and establish a parameter recommendation system based on operating condition databases. Current research mostly focuses on single-form textures such as grooves and dimples, while exploration of the application of composite and bionic textures in hydrodynamic thrust bearings is relatively scarce. Future research should comprehensively consider the intrinsic correlations between material properties, operating conditions, and texture parameters, and deepen studies on the regulation mechanisms of textures on lubrication performance.

Declaration of competing interests

The authors have no competing interests to declare that are relevant to the content of this article.

References

[1] Zhang G H, Huang M, Chen G L, Li J S, Liu Y, He J G, Zheng Y Q, Tang S W, Cui H L. Design and optimization of fluid lubricated bearings operated with extreme working performances—a comprehensive review. *Int. J. Extreme Manuf.* **6**(2): 022010 (2024)

[2] Lin X H, Jiang S Y, Zhang C B, Liu X. Thermohydrodynamic analysis of high speed water-lubricated spiral groove thrust bearing considering effects of cavitation, inertia and turbulence. *Tribol. Int.* **119**: 645-658 (2018)

[3] Lin X H, Jiang S Y, Zhang C B, Liu X. Thermohydrodynamic analysis of high-speed water-lubricated spiral groove thrust bearing using cavitating flow model. *J. Tribol.* **140**(5): 051703 (2018)

[4] Medeiros N V, Macêdo E N, Magno R N O, Blanco C J C, Quaresma J N N. Integral transform solution for the analysis of hydrodynamic lubrication of thrust bearings. *Ind. Lubr. Tribol.* **69**(6): 1074-1084 (2017)

[5] Glavatskih S, DeCamillo S. Influence of oil viscosity grade on thrust pad bearing operation. *Proc. Inst. Mech. Eng., Part J* **218**(5): 401-412 (2004)

[6] Bhat J A, Harmain G A, Najar F A. Addressing thermal challenges in hydrodynamic bearings: A contemporary review of strategies and technologies. *Proc. Inst. Mech. Eng., Part J*: 13506501241290101 (2024)

[7] Cao Y. Lubrication performance and dynamic performance analysis and experimental study of tilting pad bearing of gas turbine shaft system. Master Thesis. Xi'an University of Technology: Xi'an University of Technology, 2024

[8] Dai H M, Xiang G, Wang J X, Guo J, Wang C, Jia H. Study on time-varying mixed lubrication performance of microgroove journal-thrust coupled bearing under water lubrication. *Ind. Lubr. Tribol.* **74**(2): 265-273 (2022)

[9] Deng X. A mixed zero-equation and one-equation turbulence model in fluid-film thrust bearings. *J. Tribol.* **146**(3): 034101 (2024)

[10] Wang C C, Lin J T. Numerical study of hydrodynamic herringbone-grooved journal bearings combined with thrust bearings considering thermal effects. *J. Mech.* **38**: 13-21 (2022)

[11] Zhang X L, Yin Z W, Jiang D, Gao G Y. The design of hydrodynamic water-lubricated step thrustbearings using CFD method. *Mech. Ind.* **15**(3): 197-206 (2014)

[12] Bhat J A, Harmain G A, Najar F A. Alleviating thermal challenges in hydrodynamic bearings: A novel approach through thrust bearing pads with embedded cooling circuitry and deep recess. *Tribol. Int.* **194**: 109438 (2024)

[13] Nascimento A R, Chromik R R, Schulz R. Mechanical properties and wear resistance of industrial bearing liners in concentrated boundary-lubricated sliding. *Wear* **477**: 203806 (2021)

[14] Zhang D Y, Ho J K, Dong G N, Zhang H, Hua M. Tribological properties of Tin-based Babbitt bearing alloy with polyurethane coating under dry and starved lubrication conditions. *Tribol. Int.* **90**: 22-31 (2015)

[15] Song Y, Ren X, Gu C W, Li X S. Experimental and numerical studies of cavitation effects in a tapered land thrust bearing. *J. Tribol.* **137**(1): 011701 (2015)

[16] Wang B, Ouyang W, Wang S T, Sheng C X, He T, Yan Z Y. Load Carrying Capacity Enhancing Design and Lubrication Investigation of the Magnetic-Water Double Suspension Elastic Support Thrust Bearing. *Lubricants* **11**(9): 401 (2023)

[17] Li Y H, Wu D C, Sun X Z, Ma K, Shen J. Characteristic Analysis of Thrust Bearing with Circular Elastic Metal Plastic Pad. *Journal of Harbin University of Science and Technology* **25**(05): 113-119 (2020) (in Chinese)

[18] Yu C H, Zhu J, Zhang Y B, Huang S, Feng K. PEEK Composites and Their Application in Wind Turbine Sliding Bearings. *Bearing* (6): 20-25+76 (2023) (in Chinese)

[19] Bhat J A, Harmain G A, Wani M F, Sehgal R, Najar F A. Performance enhancement of hydrodynamic thrust bearings: Investigating cooling strategies, deep recesses, and textured surfaces. *Tribol. Int.* **211**: 110877 (2025)

[20] He H J, Liu H X, Wang X Z, Deng L M, Han Y L. Effect of ultrafast laser manufacturing errors on the tribological properties of micro thrust textured bearing. *Ind. Lubr. Tribol.*: (2025)

[21] Dai Q W, Huang W, Wang X L, Khonsari M M. Directional interfacial motion of liquids: Fundamentals, evaluations, and manipulation strategies. *Tribol. Int.* **154**: 106749 (2021)

[22] Tower B. First report on friction experiments. *Proceedings of the institution of mechanical engineers* **34**(1): 632-659 (1883)

[23] Reynolds O. IV. On the theory of lubrication and its application to Mr. Beauchamp tower's experiments, including an experimental determination of the viscosity of olive oil. *Philos. Trans. R. Soc. London* **177**: 157-234 (1886)

[24] Christopherson D G. A new mathematical method for the solution of film lubrication problems. *Proceedings of the Institution of Mechanical Engineers* **146**(1): 126-135 (1941)

[25] Zienkiewicz O C. Temperature distribution within lubricating films between parallel bearing surfaces and its effect on the pressures developed. In Proc. Conference on Lubrication and Wear, London, UK, 1957: 135-141

[26] Sternlicht B. Energy and Reynolds considerations in thrust bearing analysis. In The Inst. of Mech. Eng., Conf. on Lub. and Wear, London/England, 1957:

[27] Dowson D, Hudson J. Thermohydrodynamic analysis of the infinite slider bearing: Part I, the plane inclined slider bearing. *Proc IMechE* **181**(115): 34-44 (1963)

[28] Dowson D. Thermo-hydrodynamic analysis of the infinite slide-bearing: part II, the parallel-surface bearing. In Proc IMechE, 1963:

[29] Huebner K H. A three-dimensional thermohydrodynamic analysis of sector thrust bearings. *ASLE Trans.* **17**(1): 62-73 (1974)

[30] Kim K W, Tanaka M, Hori Y. A three-dimensional analysis of thermohydrodynamic performance of sector-shaped, tilting-pad thrust bearings. *J. Lubr. Technol.* **105**(3): 406-412 (1983)

[31] Liu F. Research on lubricating property of stability condition on large-scale water turbine group. Master Thesis. Hubei (China): Huazhong University of Science and Technology, 2008

[32] Wang L, Fu Y M, Pei S Y, Xu H. Theoretical and experimental study on the axial oil film stiffness of tilting pad thrust bearings. *Tribol. Trans.* **60**(3): 419-427 (2017)

[33] Almqvist T, Glavatskikh S B, Larsson R. THD analysis of tilting pad thrust bearings—comparison between theory and experiments. *J. Tribol.* **122**(2): 412-417 (2000)

[34] Wasilczuk M. Influence of operating conditions on optimum film profile of a thrust bearing. In Proceedings of 2nd World Tribology Congress, Vienna, Austria, 2001: 1-4

[35] Jiang X L. TEHD analysis of tilting pad thrust bearing. Master Thesis. Zhejiang (China): Zhejiang University, 2011

[36] Dimond T, Younan A, Allaire P. A review of tilting pad bearing theory. *Int J Rotating Mach* **2011**(1): 908469 (2011)

[37] Wang W M, Liu B B, Zhang Y, Shao X, Allaire P E. Theoretical and experimental study on the static and dynamic characteristics of tilting-pad thrust bearing. *Tribol. Int.* **123**: 26-36 (2018)

[38] Zhai L M. Research on the vibration of the shaft system and the 3D TEHD lubrication of the thrust bearing in the pumped storage power unit. Ph.D. Thesis. Beijing (China): Tsinghua University, 2016

[39] Pajączkowski P. Simulation of transient states in large hydrodynamic thrust bearings. Gdansk (Poland): Gdańsk University of Technology, 2010

[40] Feng X K, Yang L H. Analysis on thermoelasto-hydrodynamic lubrication characteristics of tilting pad thrust bearings under heavy load. *J. Aerosp. Power* **36**(09): 1861-1870 (2021) (in Chinese)

[41] Dong S X, Ma Q S. Thermoelastohydrodynamics analysis and size effect of large heavy thrust bearing. *Lubr. Eng.* **39**(08): 108-111+118 (2014) (in Chinese)

[42] Liu B B, Zhao W, Bai S J, Hu B, Wu K, Zhao Q J. The effect of misalignment on the performance of tilting pad thrust bearing with TEHD coupling model and turbulence model. *Adv. Mech. Eng.* **15**(6): 16878132231176191 (2023)

[43] Ma Z Y, Dong Y X. Three-dimensional thermoelastic hydrodynamic analysis of fluid film stiffness coefficient of thrust bearing. *Journal of Dalian University of Technology* (01): 101-106+112 (1991) (in Chinese)

[44] Wu D C. Thermal elastohydrodynamic lubrication performance of circular elastic metal plastic pad thrust bearing. Master Thesis. Heilongjiang (China): Harbin University of Science and Technology, 2019

[45] Sternlicht B, Carter G, Arwas E. Adiabatic analysis of elastic, centrally pivoted, sector, thrust-bearing pads. *J. Appl. Mech.* **28**(2): 179-187 (1961)

[46] Hashimoto H, Wada S. Turbulent lubrication of tilting-pad thrust bearings with thermal and elastic deformations. *J. Tribol.* **107**(1): 82-85 (1985)

[47] Ashour N. An investigation on large thrust bearings. *Military Technical College Kobry Elkobbah*: (2009)

[48] Koosha R, San Andrés L. Effect of pad and liner material properties on the static load performance of a tilting pad thrust bearing. *J. Eng. Gas Turbines Power* **141**(12): 121007 (2019)

[49] Koosha R, Andrés L S. A Model for Tilting Pad Thrust Bearings Operating With Reduced Flow Rate—Do Benefits Outweigh Risks? *J. Eng. Gas Turbines Power* **144**(2): 021026 (2022)

[50] Wang J L, Cao Y, Sun W Y, Chen R L, Jia Q, Cui Y H. Research on the lubrication performance of circular tilting pad thrust bearings for large wind turbines. *Lubr. Sci.* **36**(6): 421-430 (2024)

[51] Glavatskih S B, Fillon M, Larsson R. The significance of oil thermal properties on the performance of a tilting-pad thrust bearing. *J. Tribol.* **124**(2): 377-385 (2002)

[52] Ezzat H, Rohde S. A study of the thermohydrodynamic performance of finite slider bearings. *J. Lubr. Technol.* **95**(3): 298-307 (1973)

[53] Castelli V, Malanoski S. Method for solution of lubrication problems with temperature and elasticity effects: application to sector, tilting-pad bearings. *J. Lubr. Technol.* **91**(4): 634-640 (1969)

[54] Vohr J H. Prediction of the operating temperature of thrust bearings. *J. of Lubrication Tech.* **103**(1): 97-106 (1981)

[55] Ettles C, Anderson H. Three-dimensional thermoelastic solutions of thrust bearings using code Marmac1. *J. Tribol.* **113**(2): 405-412 (1991)

[56] Markin D, McCarthy D, Glavatskih S B. A FEM approach to simulation of tilting-pad thrust bearing assemblies. *Tribol. Int.* **36**(11): 807-814 (2003)

[57] Wodtke M, Fillon M, Schubert A, Wasilczuk M. Study of the influence of heat convection coefficient on predicted performance of a large tilting-pad thrust bearing. *J. Tribol.* **135**(2): 021702 (2013)

[58] Heinrichson N, Santos I F, Fuerst A. The influence of injection pockets on the performance of tilting-pad thrust bearings—part I: theory. *J. Tribol.* **129**(4): 895-903 (2007)

[59] El-Saie Y A, Fenner R. Three-dimensional thermoelastohydrodynamic analysis of pivoted pad thrust bearings Part 2: Application of theory and comparison with experiments. *P I Mech Eng C-j Mec* **202**(1): 51-62 (1988)

[60] Rotta G. Modeling of the oil film of a thrust bearing with the use of FEM. In Proceedings of the sixth doctoral seminar, Gdan 0 sk, 2003: 55-62

[61] Rotta G. Modeling of the gap between thrust bearing pads. *Tribology* **35**(4): 196 (2004)

[62] Wasilczuk M, Rotta G. Modeling lubricant flow between thrust-bearing pads. *Tribol. Int.* **41**(9-10): 908-913 (2008)

[63] Li Y L, Zhang Z H, He Y Y, Luo J B. Research on internal flow field characteristics of straight-groove texture using three-dimensional modeling. *Lubricants* **11**(8): 338 (2023)

[64] Li Q, Li B, Li X W, Xie Q T, Liu Q L, Xu W W. Study on transient performance of tilting-pad thrust bearings in nuclear pump considering fluid-structure interaction. *Nucl. Eng. Technol.* **55**(6): 2325-2334 (2023)

[65] Cao J W, Zhai L M, Luo Y Y, Ahn S-H, Wang Z W, Liu Y. Transient thermo-elasto-hydrodynamic analysis of a bidirectional thrust bearing in start-up and shutdown processes. *Eng. Comput.* **39**(4): 1511-1533 (2022)

[66] Ji Z W, Shi Y S, Da X M, Cao J W, Gong Q J, Wang Z W, Huang X X. Influence of installation deviation of thrust bearing on oil film flow of 1000 MW hydraulic turbine unit. *Water* **15**(9): 1649 (2023)

[67] Zouzoulas V, Papadopoulos C I. 3-D thermohydrodynamic analysis of textured, grooved, pocketed and hydrophobic pivoted-pad thrust bearings. *Tribol. Int.* **110**: 426-440 (2017)

[68] Wang H J, Gong R Z, Lu D P, Wu Z D, Li F C. Numerical simulation of the flow in a large-scale thrust bearing. In Fluids Engineering Division Summer Meeting, Montreal, Quebec, Canada, 2010: 173-180

[69] Shi Y S, Wu S Y, Huang X X, Liu X M. Analysis of oil film flow characteristics and lubrication performance of thrust bearing of 1000MW Hydraulic Turbine Unit. In Journal of Physics: Conference Series, Kashgar, China, 2024: 012048

[70] Mikula A M. Evaluating tilting-pad thrust bearing operating temperatures. *ASLE Trans.* **29**(2): 173-178 (1986)

[71] Ahmed S A, Fillon M, Maspeyrot P. Influence of pad and runner mechanical deformations on the performance of a hydrodynamic fixed geometry thrust bearing. *Proc. Inst. Mech. Eng., Part J* **224**(4): 305-315 (2010)

[72] Dadouche A, Fillon M, Bligoud J. Experiments on thermal effects in a hydrodynamic thrust bearing. *Tribol. Int.* **33**(3-4): 167-174 (2000)

[73] Dadouche A, Fillon M, Dmochowski W. Performance of a hydrodynamic fixed geometry thrust bearing: comparison between experimental data and numerical results. *Tribol. Trans.* **49**(3): 419-426 (2006)

[74] Grzegorz R, Michal W. CFD analysis of the lubricant flow in the supply groove of a hydrodynamic thrust bearing pad. In International Joint Tribology Conference, 2007: 307-309

[75] Pu K X, Yuan F X, Du P C, Huang B, Fei D D. Study on influence of pad surface defects on lubrication characteristics of thrust bearing. *Ann. Nucl. Energy* **203**: 110492 (2024)

[76] Zoupas L, Wodtke M, Papadopoulos C I, Wasilczuk M. Effect of manufacturing errors of the pad sliding surface on the performance of the hydrodynamic thrust bearing. *Tribol. Int.* **134**: 211-220 (2019)

[77] Pajączkowski P, Schubert A, Wasilczuk M, Wodtke M. Simulation of large thrust-bearing performance at transient states, warm and cold start-up. *Proc. Inst. Mech. Eng., Part J* **228**(1): 96-103 (2014)

[78] Wodtke M, Olszewski A, Wasilczuk M. Application of the fluid–structure interaction technique for the analysis of hydrodynamic lubrication problems. *Proc. Inst. Mech. Eng., Part J* **227**(8): 888-897 (2013)

[79] Wodtke M, Schubert A, Fillon M, Wasilczuk M, Pajączkowski P. Large hydrodynamic thrust bearing: Comparison of the calculations and measurements. *Proc. Inst. Mech. Eng., Part J* **228**(9): 974-983 (2014)

[80] Zhai L M, Luo Y Y, Wang Z W, Liu X. 3D Two-way coupled TEHD analysis on the lubricating characteristics of thrust bearings in pump-turbine units by combining CFD and FEA. *Chin J Mech Eng-En* **29**(1): 112-123 (2016)

[81] Zhai L M, Luo Y Y, Liu X, Chen F N, Xiao Y X, Wang Z W. Numerical simulations for the fluid-thermal-structural interaction lubrication in a tilting pad thrust bearing. *Eng. Comput.* **34**(4): 1149-1165 (2017)

[82] Huang B, Wu Z L, Wu Z D, Jiao L, Wang L Q. Effects of support structure on lubricating properties of bi-directional thrust bearings. *J. Drain. Irri. Mach. Eng.* **30**(06): 690-694 (2012) (in Chinese)

[83] Huang B, Wu Z D, Wu J L, Wang L Q. Numerical and experimental research of bidirectional thrust bearings used in pump-turbines. *Proc. Inst. Mech. Eng., Part J* **226**(9): 795-806 (2012)

[84] Wu Z D, Zhang H, Wu J L, Liu P A. Study of thrust bearing with teflon layer for large hytro-generators. *Lubr. Eng.* **40**(01): 106-109 (2015) (in Chinese)

[85] Wu Z D, Wu J L. Design and Thermo-elastic-hydrodynamic lubricating performance analysis of bi-directional thrust bearing. *Larg. Electr. Mach. Hydra. Turb.* (06): 26-28+32 (2010) (in Chinese)

[86] Zhang R J. Study on thrust bearing design of canned motor for new type nuclear main pump. Master Thesis. Heilongjiang (China): Harbin Institute of Technology, 2017

[87] Massocchi D, Lecis N, Lattuada M, Scaglia D, Chatterton S, Pennacchi P. Friction and wear performance of polyether ether ketone (PEEK) polymers in three lubrication regimes. *Friction* **12**(4): 670-682 (2024)

[88] Chen T Y, Ji J, Fu Y H, Tian P L, Zhou J P, Yang X P. Tribological analysis of picosecond laser partially textured thrust bearings with circular grooves machined: Theory and experiment. *Proc. Inst. Mech. Eng., Part J* **236**(1): 105-122 (2022)

[89] Xiao N, Khonsari M. Improving bearings thermal and tribological performance with built-in heat pipe. *Tribol. Lett.* **57**(3): 31 (2015)

[90] Suh M, Chae Y, Kim S, Hinoki T, Kohyama A. Effect of geometrical parameters in micro-grooved crosshatch pattern under lubricated sliding friction. *Tribol. Int.* **43**(8): 1508-1517 (2010)

[91] Du H F, Hou Z B, Tang Z R, Yao Z Q. Wear mechanism and three-phase synergistic effect of self-mated SiC/Si/graphite composites in unlubricated sliding. *Wear* **564**: 205674 (2025)

[92] Lu Y S, Liu Y M, Wang J, Liu H P. Tribological performance of dimpled thrust bearings with phyllotactic patterns. *Wear* **346**: 108-115 (2016)

[93] Dong C L, Yuan C Q, Xu A J, Bai X Q, Tian Y. Rippled polymer surface generated by stick–slip friction. *Langmuir* **35**(7): 2878-2884 (2019)

[94] Li Y L, Zhang Z H, He Y Y, Luo J B. Optimization of surface texture distribution on the thrust bearing using the mass-conserving cavitation boundary condition: Theory and experiments. *Tribol. Int.* **194**: 109551 (2024)

[95] Lan P X, Polychronopoulou K, Zhang Y F, Polycarpou A A. Three-body abrasive wear by (silica) sand of advanced polymeric coatings for tilting pad bearings. *Wear* **382**: 40-50 (2017)

[96] Harika E, Bouyer J, Fillon M, Helene M. Measurements of lubrication characteristics of a tilting pad thrust bearing disturbed by a water-contaminated lubricant. *Proc. Inst. Mech. Eng., Part J* **227**(1): 16-25 (2013)

[97] Henry Y, Bouyer J, Fillon M. An experimental hydrodynamic thrust bearing device and its application to the study of a tapered-land thrust bearing. *J. Tribol.* **136**(2): 021703 (2014)

[98] Henry Y, Bouyer J, Fillon M. An experimental analysis of the hydrodynamic contribution of textured thrust bearings during steady-state operation: A comparison with the untextured parallel surface configuration. *Proc. Inst. Mech. Eng., Part J* **229**(4): 362-375 (2015)

[99] Henry Y, Bouyer J, Fillon M. Experimental analysis of the hydrodynamic effect during start-up of fixed geometry thrust bearings. *Tribol. Int.* **120**: 299-308 (2018)

[100] Bouyer J, Wodtke M, Fillon M. Experimental research on a hydrodynamic thrust bearing with hydrostatic lift pockets: Influence of lubrication modes on bearing performance. *Tribol. Int.* **165**: 107253 (2022)

[101] Xie Q T, Du P C, Fei D D, Li Q, Li X W, Li B, Liu Z Z. Simulation and experimental study of the effect of thrust bearing with worn pads on lubrication performance. *Ann. Nucl. Energy* **206**: 110583 (2024)

[102] Fais C, Ali M, Yasko I. Hydrodynamic thrust bearing test rig with novel bearing alignment system. *J. Tribol.* **146**(12): 124101 (2024)

[103] Liu W, Liu Y J, Yu Q, Li Q C. Shaft axial vibration characteristic analysis and loading device optimization at test platform. *Manuf. Auto.* **37**(15): 36-39 (2015) (in Chinese)

[104] Liang X X, Yan X P, Ouyang W, Liu Z L. Experimental research on tribological and vibration performance of water-lubricated hydrodynamic thrust bearings used in marine shaft-less rim driven thrusters. *Wear* **426**: 778-791 (2019)

[105] Zhang C, Xie D C, Huang Q W, Wang Z H. Experimental research on the vibration of ship propulsion shaft under hull deformation excitations on bearings. *Shock Vib.* **2019**(1): 4367061 (2019)

[106] Myers K, Jenson S, Brooksbank M, Ali M, Alam K, Choi J, Wilhelm J, Gillespie J, Walker R. Performance evaluation of thrust washer bearings using a customized bench scale test rig. In ASME International Mechanical Engineering Congress and Exposition, Phoenix, Arizona, USA, 2016: V04AT05A054

[107] Fais C, Ali M, Yasko I, Walker R, Lutfullaeva A. Experimental Performance Evaluation of Fixed-Geometry Hydrodynamic Thrust Bearings With Variable Taper Depths. In ASME International Mechanical Engineering Congress and Exposition, 2021: V003T003A065

[108] Fais C, Yasko I, Lutfullaeva A, Ali M, Walker R. Experimental investigation of fixed-geometry thrust bearing taper geometry on critical operating parameters. In ASME International Mechanical Engineering Congress and Exposition, 2022: V003T003A055

[109] Li Q, Xie Q T, Du P C, Fei D D, Li X W, Li B, Liu Z Z. Experimental study on scaled-down pads for nuclear main pump thrust bearing. *Ann. Nucl. Energy* **198**: 110297 (2024)

[110] Wang N M, Liu W R, Teng J G, Wei G J, Dai H L, Zhao X Y, Liao H, Ren G H, Tang Y A, Han Z Z. Research on multi-functional test bench for full sized largge thrust bearings of nuclear main pump. *Pump Technol.* (05): 49-52 (2024) (in Chinese)

[111] Li P, Liu X J. Experimental study on thrust bearing oil cooler of nuclear main pump. *Mech. Manag. Develop.* **40**(02): 1-4 (2025) (in Chinese)

[112] Li P, Liu X J. Structural optimization and experimental study on thrust bearing of nuclear main pump. *Mech. Res. & Appli.* **38**(01): 26-28+33 (2025) (in Chinese)

[113] Li P, Liu X J. Development of a New Type of Vertical Thrust Plain Bearing. *Mech. Manag. Develop.* **38**(09): 17-19+24 (2023) (in Chinese)

[114] Tao S J, Liu X J, Zhang Y B, Zhou X J, Li P, Su X S. Analysis on structural optimization of the main and auxiliary elastic plates of clear min pmp barings. *Fluid Mach.* **47**(11): 46-48+65 (2019) (in Chinese)

[115] Guo A N, Wang X J, Jin J, Hua D Y, Hua Z K. Experimental test of static and dynamic characteristics of tilting-pad thrust bearings. *Adv. Mech. Eng.* **7**(7): 1687814015593878 (2015)

[116] Zhu J, Zhang K, Feng K. Experimental measurement of oil film thickness distribution in titling-pad thrust bearings by ultrasonic piezoelectric elements. *J. Vib. Eng. Technol.* **9**(6): 1335-1346 (2021)

[117] Wang Z C, Liu Y, Wang Y C, Liu X F, Wang Y M. Influence of squeezing and interface slippage on the performance of water‐lubricated tilting‐pad thrust bearing during start‐up and shutdown. *Lubr. Sci.* **30**(4): 137-148 (2018)

[118] Wasilczuk M, Wodtke M. Experimental study on the feasibility of alternative materials for tilting pad thrust bearings operating in transition to mixed friction. *Friction* **12**(4): 812-822 (2024)

[119] Zhang X L, Gao G Y, Yin Z W, Wang Y Z, Gao C. Numerical analysis and experimental research on load carrying capacity of water-lubricated tilting-pad thrust bearings. *Mech. Ind.* **19**(2): 201 (2018)

[120] Liu X, Li R, Zhang W P, Liu Z C. Bearing load measurement in condition of large shafting operation. *Experi. Technol. and Manag.* **37**(10): 67-71 (2020) (in Chinese)

[121] Ou Y W, Cheng Q C, Wang L, Jin Y. Distributed dynamics characteristics of water-lubricatted stern bearing under offset load. *J. Traffic Transp. Eng.* **19**(02): 92-100 (2019) (in Chinese)

[122] Zhang Z, Ouyang W, Liang X X, Yan X P, Yuan C Q, Zhou X C, Guo Z W, Dong C L, Liu Z L, Jin Y. Review of the evolution and prevention of friction, wear, and noise for water-lubricated bearings used in ships. *Friction* **12**(1): 1-38 (2024)

[123] Yang S F, Li C, Jiang M L, Pei S Y. A study of inlet temperature models of a large size tilting thrust bearing comparison between theory and experiment. *Tribol. Int.* **140**: 105881 (2019)

[124] Jia Y P, Dou P, Zheng P, Wu T H, Yang P P, Yu M, Reddyhoff T. High-accuracy ultrasonic method for in-situ monitoring of oil film thickness in a thrust bearing. *Mech. Syst. Sig. Process.* **180**: 109453 (2022)

[125] Jia L T. Research on the design and application of thrust bearing for the generator of the Left Bank of WDD Hydropower Station. Master Thesis. Sichuan (China): Sichuan University, 2021

[126] Majumdar B, Pai R, Hargreaves D. Analysis of water-lubricated journal bearings with multiple axial grooves. *Proc. Inst. Mech. Eng., Part J* **218**(2): 135-146 (2004)

[127] Wang N, Meng Q F. Research on wireless nondestructive monitoring method for film pressure of water-lubricated bearing. *Ind. Lubr. Tribol.* **67**(4): 349-358 (2015)

[128] Xie Z C. Research on optical fiber measurement method and system of thrust pad pressure distribution of thrust sliding bearing. Master Thesis. Hubei (China): Wuhan University of Technology, 2021

[129] Youssef A, Matthews D, Guzzomi A, Pan J. Measurement of pressure fluctuations inside a model thrust bearing using PVDF sensors. *Sensors* **17**(4): 878 (2017)

[130] Liu H, Yu Q, Tan Y G, Xu W J, Huang B, Xie Z C, Mao J. Feasibility study on temperature distribution measurement method of thrust sliding bearing bush based on FBG quasi-distributed sensing. *Sensors* **19**(14): 3245 (2019)

[131] Glavatskih S. A method of temperature monitoring in fluid film bearings. *Tribol. Int.* **37**(2): 143-148 (2004)

[132] Wei W, Wang L F, Yu J W, Gao G H, Yu X F. Infrared measurement and reconstruction research on transient temperature field of spherical plain bearings. *Bearing* (03): 43-47 (2016) (in Chinese)

[133] McCarthy D, Glavatskih S, Sherrington I. Oil-film thickness and temperature measurements in PTFE and babbitt faced tilting-pad thrust bearings. *Proc. Inst. Mech. Eng., Part J* **219**(3): 179-185 (2005)

[134] Liu H C, Guo F, Zhang B B, Wong P L. Behavior of hydrodynamic lubrication films under non-steady state speeds. *Tribol. Int.* **93**: 347-354 (2016)

[135] Sun X G, Dai J M, Cong D C, Chu Z X. Development of oil film thickness measuring system for thrust bearing. *ACTA Meteorol. Sin.* **24**(02): 92-94 (2003) (in Chinese)

[136] Fowell M, Myant C, Spikes H, Kadiric A. A study of lubricant film thickness in compliant contacts of elastomeric seal materials using a laser induced fluorescence technique. *Tribol. Int.* **80**: 76-89 (2014)

[137] Chao Q, Zhang J H, Xu B, Wang Q N. Multi-position measurement of oil film thickness within the slipper bearing in axial piston pumps. *Measurement* **122**: 66-72 (2018)

[138] Cen H, Lugt P M. Film thickness in a grease lubricated ball bearing. *Tribol. Int.* **134**: 26-35 (2019)

[139] Jiang S Y, Li S H, Zhou F D, Lin X H. Study on Lubricating Performance of the Bubbly Oil Under High Shear Rate—Part 2: Application Study in High-Speed Bearing. *J. Tribol.* **145**(8): 084103 (2023)

[140] Poll G, Gabelli A. Formation of lubricant film in rotary sealing contacts: part II—a new measuring principle for lubricant film thickness. *J. Tribol.* **114**(2): 290-296 (1992)

[141] Dwyer-Joyce R, Drinkwater B, Donohoe C. The measurement of lubricant–film thickness using ultrasound. *Proc. R. Soc. A* **459**(2032): 957-976 (2003)

[142] Jiao J P, Liu W H, Zhang J, Zhang Q, He C F, Wu B. Time–frequency analysis for ultrasonic measurement of liquid-layer thickness. *Mech. Syst. Sig. Process.* **35**(1-2): 69-83 (2013)

[143] Dou P, Wu T H, Peng Z X. A time-domain ultrasonic approach for oil film thickness measurement with improved resolution and range. *Meas. Sci. Technol.* **31**(7): 075006 (2020)

[144] Liang P, Kong L S, Guo F, Sun W, Jiang F L. Real-time measurement of dynamic film thickness via ultrasonic technology. *Friction* **13**(5): (2025)

[145] Guo Z X, He Y Y, Lu X C. Tribological performance of Tin-based white metal ZSnSb8Cu4. *Lubr. Eng.* **39**: 5-10 (2014) (in Chinese)

[146] Zhou F M, Zhang Q Y, Shi M X, Guo J W, Li H. The effect of TIG arc brazing current on interfacial structure and bonding strength of tin-based babbit. *J. Adhes. Sci. Technol.* **31**(21): 2312-2322 (2017)

[147] Wang X B, Yin Z W, Chen Y H. Study on fatigue strength of SnSb11Cu6 babbitt-steel bimetal sliding bearing material prepared by MIG brazing. *Mech. Ind.* **21**(1): 106 (2020)

[148] Brown A L, Medley J B, Ferguson J H. Spring-supported thrust bearings used in hydroelectric generators: Limit ofhydrodynamic lubrication. *Tribol. Ser.* **38**: 261-274 (2000)

[149] Inc K. Equilizing Thrust Bearings-Comprehensive Design Guide. Kingsbury. Inc, 2011

[150] Leopard A J. Tilting pad bearings-linits of operation. *Lubr. Eng* **32**: 637-644 (1976)

[151] Wasilczuk M. Friction and lubrication of large tilting-pad thrust bearings. *Lubricants* **3**(2): 164-180 (2015)

[152] Wang W G, Cai L, Li W, Liu C B, Wang Z M, Che H Y. Research progress of composite thrust pads in oil lubricated bearings. *Larg. Electr. Mach. Hydra. Turb.* (02): 39-45 (2019) (in Chinese)

[153] Ettles C, Knox R, Ferguson J, Horner D. Test results for PTFE-Faced thrust pads, with direct comparison against Babbitt-faced pads and correlation with analysis. *J. Tribol.* **125**(4): 814-823 (2003)

[154] Nie Z, Li G P, Wang X J, Jiao Y D, Hua Z K, Yu G Y. Dynamic experimental research of PTFE-Faced pad thrust bearings. *Tribol. Lett.* **62**(1): 8 (2016)

[155] Simmons G F, Cerda Varela A, Santos I F, Glavatskih S. Dynamic characteristics of polymer faced tilting pad journal bearings. *Tribol. Int.* **74**: 20-27 (2014)

[156] Wang S, Tan Q C, Kou Z Q. Thermal elastohydrodynamic lubrication analysis of large scale composite thrust bearing with sector pad faced by PTFE. *Ind. Lubr. Tribol.* **68**(1): 67-75 (2016)

[157] Fang J H, Wang J G, Zhao Z Q, Chen Z X, Yan J L. Comparative analysis on thrust bearings with PTFE pad and babbitt alloy pad based on TEHD modeling. *Bearing* (04): 29-32+41 (2012) (in Chinese)

[158] Butler J. Thrust block performance improvements using polymer lined tilting pads. In Conference Proceedings of INEC, 2022:

[159] Glavatskih S, Fillon M. TEHD analysis of thrust bearings with PTFE-faced pads. *J. Tribol.* **128**(1): 49-58 (2006)

[160] Fillon M, Glavatskih S. PTFE-Faced centre pivot thrust pad bearings: Factors affecting TEHD performance. *Tribol. Int.* **41**(12): 1219-1225 (2008)

[161] Machino S, Shinkai S, Matsueda T, Mizobe K, Kida K. Observation of wear around surface crack of PEEK thrust bearing under rolling contact fatigue in water. In Journal of Physics: Conference Series, 2024: 012007

[162] Sumi Y, Sano T, Shinohara T, Tochitani N, Otani Y, Yamashita K, Nakano T. Development of thrust bearings with high specific load. In Turbo Expo: Power for Land, Sea, and Air, Düsseldorf, Germany, 2014: V01BT27A044

[163] Zhou J, Blair B, Argires J, Pitsch D. Experimental performance study of a high speed oil lubricated polymer thrust bearing. *Lubricants* **3**(1): 3-13 (2015)

[164] Bouyer J, Fillon M. Experimental measurement of the friction torque on hydrodynamic plain journal bearings during start-up. *Tribol. Int.* **44**(7-8): 772-781 (2011)

[165] Wasilczuk M, Wodtke M, Braun W. Centrally pivoted tilting pad thrust bearing with carbon-based coated collar—Experimental results of low-and medium-speed operation. *Tribol. Trans.* **58**(5): 882-893 (2015)

[166] Ricci R, Chatterton S, Pennacchi P E L, Vania A T. Multiphysics modeling of a tilting pad thrust bearing with polymeric layered pads-Modélisation multi physique d'un butée à patins oscillants avec le revêtement enpolymères. *Re. Public@Polimi*: 1-10 (2011)

[167] Wodtke M, Wasilczuk M. Evaluation of apparent Young' s modulus of the composite polymer layers used as sliding surfaces in hydrodynamic thrust bearings. *Tribol. Int.* **97**: 244-252 (2016)

[168] Ma F L, Zeng Z X, Gao Y M, Liu E Y, Xue Q J. Research status and progress of bionic surface drag reduction. *China Surf. Eng.* **29**(01): 7-15 (2016) (in Chinese)

[169] Xu Q, Wan Y Y, Hu T S, Liu T X, Tao D S, Niewiarowski P H, Tian Y, Liu Y, Dai L M, Yang Y Q. Robust self-cleaning and micromanipulation capabilities of gecko spatulae and their bio-mimics. *Nat. Commun.* **6**(1): 8949 (2015)

[170] Dai Q W, Du C X, Huang W, Wang X L. Regulation of Liquid Self-Transport Through Architectural-Thermal Coupling: Transitioning From Free Surfaces to Open Channels. *ADVANCED SCIENCE* **12**(15): 202412483 (2025)

[171] Dai Q W, Chen L, Pan J B, Shi L P, Liu D M, Huang W, Wang X L. Rapid surface texturing to achieve robust superhydrophobicity, controllable droplet impact, and anti-frosting performances. *Friction* **12**(2): 291-304 (2024)

[172] Cai Y K, Aslam J, Xue J, Song Q H, Ma H F, Liu Z Q. Enhancement of tribological performance with Laser surface texturing: A review. *Proc. Inst. Mech. Eng., Part J*: 13506501251330449 (2024)

[173] Kovalchenko A, Ajayi O, Erdemir A, Fenske G, Etsion I. The effect of laser surface texturing on transitions in lubrication regimes during unidirectional sliding contact. *Tribol. Int.* **38**(3): 219-225 (2005)

[174] Wang Z Q, Ye R H, Xiang J B. The performance of textured surface in friction reducing: A review. *Tribol. Int.* **177**: 108010 (2023)

[175] Nsilani Kouediatouka A, Ma Q, Liu Q, Mawignon F J, Rafique F, Dong G N. Design methodology and application of surface texture: A review. *Coatings* **12**(7): 1015 (2022)

[176] Zhao T, Wang Y Q, Li M J, Zhu Y L, He Y. Research progress on improvement of tribological properties of materials by surface micro-texture and thermal diffusion technology. *Surf. Technol.* **52**(08): 89-103 (2023) (in Chinese)

[177] Zhao L X, Zhang B L, Liu Y, Liu Y. State of the art for Improving tribological performance based on of surface texturing technology. *Tribology* **42**(1): 202-224 (2022) (in Chinese)

[178] Dobrica M, Fillon M. About the validity of Reynolds equation and inertia effects in textured sliders of infinite width. *Proc. Inst. Mech. Eng., Part J* **223**(1): 69-78 (2009)

[179] Gropper D, Wang L, Harvey T J. Hydrodynamic lubrication of textured surfaces: A review of modeling techniques and key findings. *Tribol. Int.* **94**: 509-529 (2016)

[180] Papadopoulos C I, Nikolakopoulos P G, Kaiktsis L. Evolutionary optimization of micro-thrust bearings with periodic partial trapezoidal surface texturing. *J. Eng. Gas Turbines Power* **133**(1): 012301 (2011)

[181] Fouflias D G, Charitopoulos A G, Papadopoulos C I, Kaiktsis L, Fillon M. Performance comparison between textured, pocket, and tapered-land sector-pad thrust bearings using computational fluid dynamics thermohydrodynamic analysis. *Proc. Inst. Mech. Eng., Part J* **229**(4): 376-397 (2015)

[182] Gropper D, Harvey T J, Wang L. Numerical analysis and optimization of surface textures for a tilting pad thrust bearing. *Tribol. Int.* **124**: 134-144 (2018)

[183] Chalkiopoulos M, Charitopoulos A, Fillon M, Papadopoulos C I. Effects of thermal and mechanical deformations on textured thrust bearings optimally designed by a THD calculation method. *Tribol. Int.* **148**: 106303 (2020)

[184] Yun J Q, Liu B C. Tribological behavior of textured polycrystalline diamond compact for thrust bearings using the surface morphology of dung beetles as an inspiration. *Tribol. Int.* **199**: 109936 (2024)

[185] Yu H W, Wang X L, Zhou F. Geometric shape effects of surface texture on the generation of hydrodynamic pressure between conformal contacting surfaces. *Tribol. Lett.* **37**(2): 123-130 (2010)

[186] Atwal J C, Pandey R K. Performance improvement of water-lubricated thrust pad bearing operating with the turbulent flow using a new micro-pocket design. *Tribol. Int.* **154**: 106738 (2021)

[187] Atwal J C, Pandey R K. Performance analysis of thrust pad bearing using micro-rectangular pocket and bionic texture. *Proc. Inst. Mech. Eng., Part J* **235**(6): 1232-1250 (2021)

[188] Jiang S Y, Liu P F, Lin X H. Study on static characteristics of water-lubricated textured spiral groove thrust bearing using laminar cavitating flow lubrication model. *J. Tribol.* **144**(4): 041803 (2022)

[189] Ran H F, Dai P, Yan S P, Wang F T, Yao X J, Wang J P, Zuo G Z. Flow mechanisms and lubrication performance of water-lubricated thrust bearings with herringbone grooves. *Lubricants* **10**(8): 182 (2022)

[190] Brizmer V, Kligerman Y, Etsion I. A laser surface textured parallel thrust bearing. *Tribol. Trans.* **46**(3): 397-403 (2003)

[191] Etsion I, Halperin G, Brizmer V, Kligerman Y. Experimental investigation of laser surface textured parallel thrust bearings. *Tribol. Lett.* **17**(2): 295-300 (2004)

[192] Marian V G, Gabriel D, Knoll G, Filippone S. Theoretical and experimental analysis of a laser textured thrust bearing. *Tribol. Lett.* **44**(3): 335 (2011)

[193] Fu G, Untaroiu A. The influence of surface patterning on the thermal properties of textured thrust bearings. *J. Tribol.* **140**(6): 061706 (2018)

[194] Gherca A, Fatu A, Hajjam M, Maspeyrot P. Influence of surface texturing on the hydrodynamic performance of a thrust bearing operating in steady-state and transient lubrication regime. *Tribol. Int.* **102**: 305-318 (2016)

[195] Kumar V, Sharma S C. Performance analysis of rough surface hybrid thrust bearing with elliptical dimples. *Proc. Inst. Mech. Eng., Part J* **235**(6): 1101-1113 (2021)

[196] Panigrahi D K, Sarangi M. Tribological performance of positive deterministic textured surfaces in parallel sliding lubricated contacts: effect of texture size and height. *Proc. Inst. Mech. Eng., Part J* **234**(12): 1908-1925 (2020)

[197] Atwal J C, Pandey R K. Influence of new surface micro-structures on the performance behaviours of fluid film tilting pad thrust bearings. *Proceedings of the Institution of Mechanical Engineers, Part C: Journal of Mechanical Engineering Science* **236**(6): 3111-3134 (2022)

[198] Atwal J C, Pandey R K. Film thickness and friction investigations in a fluid film thrust bearing employing a new conceived micro-texture on pads. *J. Tribol.* **143**(6): 061801 (2021)

[199] Wang W, He Y Y, Zhao J, Li Y, Luo J B. Numerical optimization of the groove texture bottom profile for thrust bearings. *Tribol. Int.* **109**: 69-77 (2017)

[200] Fouflias D G, Charitopoulos A G, Papadopoulos C I, Kaiktsis L. Thermohydrodynamic analysis and tribological optimization of a curved pocket thrust bearing. *Tribol. Int.* **110**: 291-306 (2017)

[201] Zhang H, Liu Y, Hua M, Zhang D Y, Qin L G, Dong G N. An optimization research on the coverage of micro-textures arranged on bearing sliders. *Tribol. Int.* **128**: 231-239 (2018)

[202] Zhang H, Liu Y, Hafezi M, Hua M, Dong G N. A distribution design for circular concave textures on sectorial thrust bearing pads. *Tribol. Int.* **149**: 105733 (2020)

[203] Wang W, He Y Y, Zhao J, Mao J Y, Hu Y T, Luo J B. Optimization of groove texture profile to improve hydrodynamic lubrication performance: Theory and experiments. *Friction* **8**(1): 83-94 (2020)

[204] Li Y L, Sun D N, He Y Y, Luo J B. Coupled optimization of groove texture for parallel ring–ring friction pairs: theory and experiments. *Tribol. Lett.* **70**(2): 53 (2022)

[205] Yu X D, Shi G Q, Gao W C, Yang X Y. Effects of differently shaped textures on the tribological properties of static and dynamic pressure thrust bearings and multiobjective optimization. *Ind. Lubr. Tribol.* **76**(6): 769-787 (2024)

[206] Yu X D, Shi G Q, Jiang H, Dai R C, Jia W T, Yang X Y, Gao W C. Effect of texture parameters on the lubrication performance of static and dynamic pressure thrust bearings and multi-objective optimization. *Ind. Lubr. Tribol.* **76**(4): 526-536 (2024)

[207] Yu X D, Shi G Q, Jiang H, Lan Z Y, Lin Y L. Effect and optimization of triangular textures on lubrication performance of hydrostatic and hydrodynamic hybrid thrust bearings. *J. Braz. Soc. Mech. Sci. Eng.* **46**(8): 482 (2024)

[208] Yu X D, Shi G Q, Gao W C, Yang X Y. Effect of surface square textures on the physical field of static and dynamic pressure thrust bearings and multi-objective optimization. *Ind. Lubr. Tribol.* **76**(10): 1294-1307 (2024)

[209] Lyu B, Jing L L, Meng X H, Liu R C. Texture optimization and verification for the thrust bearing used in rotary compressors based on a transient tribo-dynamics model. *J. Tribol.* **144**(8): 081801 (2022)

[210] Tang H S, Ren Y, Kumar A. Optimization tool based on multi-objective adaptive surrogate modeling for surface texture design of slipper bearing in axial piston pump. *Alexandria Eng. J.* **60**(5): 4483-4503 (2021)

[211] Li Q, Wang Y J, Zhang S, Xu W W, Bai L, Wang Z B. Investigation and optimization of textured thrust bearings with spirally distributed dimples using multi-objective optimization method. *Ind. Lubr. Tribol.* **72**(6): 749-759 (2020)

[212] Cheng Y Q, He Q, Huang W F, Liu Y, Li Y W, Li D C. HL-nets: Physics-informed neural networks for hydrodynamic lubrication with cavitation. *Tribol. Int.* **188**: 108871 (2023)

[213] Xue E C, Guo Z W, Wu Z M, Jiang S L, Huang Q R, Yuan C Q. Dual neural network for contact temperature and cooling state monitoring in water-lubricated bearings. *Measurement* **239**: 115501 (2025)

[214] Zhao Y, Guo L, Wong P P L. Application of physics-informed neural network in the analysis of hydrodynamic lubrication. *Friction* **11**(7): 1253-1264 (2023)

[215] Xi Y H, Deng J H, Li Y L. A solution for finite journal bearings by using physics-informed neural networks with both soft and hard constrains. *Ind. Lubr. Tribol.* **75**(5): 560-567 (2023)